Toxicology 448 (2021) 152637

Contents lists available at ScienceDirect

Toxicology

journal homepage: www.elsevier.com/locate/toxicol

Characterization of application scenario-dependent pharmacokinetics and pharmacodynamic properties of permethrin and hyperforin in a dynamic skin and liver multi-organ-chip model

Jochen Kühnl [a,*], Thi Phuong Tao [b], Katrin Brandmair [a], Silke Gerlach [a], Thamée Rings [a], Ursula Müller-Vieira [c], Julia Przibilla [c], Camille Genies [e], Carine Jaques-Jamin [e], Andreas Schepky [a], Uwe Marx [b], Nicola J. Hewitt [d], Ilka Maschmeyer [b]

[a] Beiersdorf AG, Unnastraße 48, D-20253, Hamburg, Germany
[b] TissUse GmbH, Oudenarder Str. 16, D-13347, Berlin, Germany
[c] Pharmacelsus GmbH, Science Park 2, D-66123, Saarbrücken, Germany
[d] Cosmetics Europe, Avenue Herrmann-Debroux 40, 1160, Auderghem, Belgium
[e] Pierre Fabre Dermo-Cosmétique, Toulouse, France

ARTICLE INFO

Keywords:
Microphysiological systems
Cosmetics
Exposure routes
Permethrin
Toxicokinetics
Toxicodynamics
Hyperforin
Skin
EpiDerm
Liver spheroids
Intra-and inter-lab reproducibility

ABSTRACT

Microphysiological systems (MPS) aim to mimic the dynamic microenvironment and the interaction between tissues. While MPS exist for investigating pharmaceuticals, the applicability of MPS for cosmetics ingredients is yet to be evaluated. The HUMIMIC Chip2 ("Chip2″), is the first multi-organ chip technology to incorporate skin models, allowing for the topical route to be tested. Therefore, we have used this model to analyze the impact of different exposure scenarios on the pharmacokinetics and pharmacodynamics of two topically exposed chemicals, hyperforin and permethrin. The Chip2 incorporated reconstructed human epidermis models (EpiDerm™) and HepaRG-stellate spheroids. Initial experiments using static incubations of single organoids helped determine the optimal dose. In the Chip2 studies, parent and metabolites were analyzed in the circuit over 5 days after application of single and repeated topical or systemic doses. The gene expression of relevant xenobiotic metabolizing enzymes in liver spheroids was measured to reflect toxicodynamics effects of the compounds in liver. The results show that 1) metabolic capacities of EpiDerm™ and liver spheroids were maintained over five days; 2) EpiDerm™ model barrier function remained intact; 3) repeated application of compounds resulted in higher concentrations of parent chemicals and most metabolites compared to single application; 4) compound-specific gene induction *e.g.* induction of CYP3A4 by hyperforin depended on the application route and frequency; 5) different routes of application influenced the systemic concentrations of both parents and metabolites in the chip over the course of the experiment; 6) there was excellent intra- and inter-lab reproducibility. For permethrin, a process similar to the excretion in a human *in vivo* study could be simulated which was remarkably comparable to the *in vivo* situation. These results support the use of the Chip2 model to provide information on parent and metabolite disposition that may be relevant to risk assessment of topically applied cosmetics ingredients.

Abbreviations: ADH, alcohol dehydrogenase; ALDH, aldehyde dehydrogenase; CVA, cis- or trans-3-(2,2 dichlorovinyl)-2,2-dimethyl-(1-cyclopropane) carboxylic acid; H&E, hematoxylin & eosin; HHSteCs, human hepatic stellate cells; LDH, lactate dehydrogenase; LLOQ, (lower limit of quantification); MPS, microphysiological systems; MTT, 3-(4,5-dimethylthiazol-2-yl)-2,5-diphenyltetrazolium bromide; PBCOOH, phenoxybenzoic acid; PBOH, 3-phenoxybenzyl alcohol; PDMS, polydimethylsiloxane; MS, mass spectrometry; MS-SIM, MS-selected ion monitoring; LC–MS-MS, Liquid Chromatography - Tandem Mass Spectrometry; TEER, trans-epithelial electrical resistance; XME, xenobiotic metabolizing enzyme.

* Corresponding author at: Beiersdorf AG, Unnastraße 48, D-20253, Hamburg, Germany.
E-mail address: Jochen.Kuehnl@Beiersdorf.com (J. Kühnl).

https://doi.org/10.1016/j.tox.2020.152637
Received 20 August 2020; Received in revised form 11 November 2020; Accepted 12 November 2020
Available online 18 November 2020
0300-483X/

1. Introduction

Non-animal methods are essential for the paradigm shift towards animal-free qualification of new compounds (Berggren et al., 2017). Guided by ethical considerations and regulatory requirements such as the cosmetics directive (EU, 2009), the cosmetics industry is developing and evaluating alternative testing strategies and methodologies. Novel *in vitro* assays, *in silico* approaches and testing strategies have been developed for several toxicological endpoints, such as skin irritation, corrosion and phototoxicity (Liebsch et al., 1997; OECD, 2019a, b; Portes et al., 2002), eye irritation and corrosion (OECD, 2017, 2018), as well as genotoxicity *via* the topical (Chapman et al., 2014; Reisinger et al., 2018) and oral routes (Reisinger et al., 2019). However, there are no validated *in vitro* systems to address systemic toxicity, resulting in a gap for the *ab initio* assessment of compounds that become bioavailable after skin permeation, oral uptake, or inhalation. In addition to the current lack of translation for the assessment of systemic toxicity following topical application *in vitro*, the assessment of distribution to the skin and subsequent toxicity following systemic exposure (*e.g.*, *via* oral administration) cannot currently be addressed using static *in vitro* models. To address these gaps, dynamic microphysiological systems (MPS) integrating 3D tissues have recently emerged as promising platforms for the *in vitro* assessment of systemic toxicity-related questions (Marx et al., 2016; Truskey, 2018; Van Ness et al., 2017). "Organs-on-chip" and "multi-organ chip" co-cultures aim to emulate the *in vivo* tissue architecture and physiology of single organs and the interactions between the different tissues, respectively. These models can provide insights into the toxicokinetic and toxicodynamic properties of chemicals. Indeed, several reports support the use of MPS for investigating the effects of systemic exposure of pharmaceuticals (Edington et al., 2018; Maass et al., 2017; Sung and Shuler, 2009). One such technology is the TissUse HUMIMIC Chip model, which can be equipped with combinations of multiple different organoids (an "organoid" is defined here as a general term to refer to a 3D tissue construct representing an organ, each representing 1:100,000 of the functional unit of the human body) in distinct compartments connected by microfluidic channels on a platform the size of a standard microscope slide (Atac et al., 2013; Hasenberg et al., 2015; Maschmeyer et al., 2015b; Materne et al., 2015; Schimek et al., 2013; Wagner et al., 2013). Directed fluid flow is driven by on-chip peristaltic micropumps, which are activated by pressured air or vacuum, resulting in a progressive lowering and raising of the 500 μm thick elastic membranes. The directed, pulsatile flow emulates *in vivo*--like conditions and ensures a sequential exposure of the tissues to the applied chemical.

While there are several examples of how the MPS models can be used to investigate drug effects (Hübner et al., 2018; Maass et al., 2017; Maschmeyer et al., 2015a; Sung and Shuler, 2009) and support its use in regulatory toxicology (Gordon et al., 2015), there are few reports describing the use of these models for use in the safety assessment of cosmetic ingredients. The main exposure route of most cosmetic ingredient is *via* the skin; therefore, the HUMIMIC technology includes the integration of a skin compartment to investigate the skin barrier function and potential "first pass" metabolism of topically applied chemicals (Hübner et al., 2018; Maschmeyer et al., 2015b; Wagner et al., 2013). In this study, we evaluated a "skin and liver" equipped HUMIMIC Chip2 (referred to as the "Chip2″), for its ability to provide biokinetic information on the application scenario-dependent differences in the bioavailability and metabolic fate of chemicals. To this end, one microfluidically-connected compartment of the Chip2 was equipped with a reconstructed human epidermal skin model and the other compartment was equipped with liver-stellate spheroids (Atac et al., 2013; Hasenberg et al., 2015; Maschmeyer et al., 2015a; b; Wagner et al., 2013). To evaluate the robustness and reproducibility of the Chip2, we selected EpiDerm™ models for skin in order to avoid donor-donor variability. EpiDerm™ models are reported to be metabolically functional in static cultures for several days (Götz et al., 2012) and exhibit metabolic characteristics similar to native human skin (Hewitt et al., 2013). Although the penetration of chemicals is reported to be higher using EpiDerm™ models than native human skin (Ackermann et al., 2010), we considered it to be a suitable model for the purposes of these studies since we were investigating inter-laboratory reproducibility. Liver spheroids were generated from a combination of HepaRG cells and human hepatic stellate cells (HHStec). There were two main reasons for the combination of non-parenchymal cells and HepaRG cells. The first was that, in our experience, the addition of HHStecs improved spheroid formation and maintained their compact and smooth spherical structure. The second was that the use of HHStecs resulted in a model that was closer to the *in vivo* liver structure than when only HepaRG cells were used. Although other non-parenchymal cells exist in the liver, the use of only one type was practically simpler and less resource intensive (thus decreasing variability across experiments). HHStecs maintain the extracellular matrix environment and store vitamin A under steady state conditions, the activation of HHStecs induces myofibroblastic features relevant for the wound healing response of the liver (Friedman, 2008) but also for the development of liver fibrosis (Higashi et al., 2017; Puche et al., 2013). HepaRG cells are considered a good alternative to human hepatocytes (Hart et al., 2010; Jetten et al., 2013), and were also used to demonstrate reproducibility. HepaRG cell-based liver spheroids have been shown to be relevant hepatic models (Ramaiahgari and Ferguson, 2019; Ramaiahgari et al., 2017; Wang et al., 2015); moreover, the 3D format and physiological flow conditions improve hepatic cell viability and functionality (Mufti et al., 1995; Park et al., 2008; Tilles et al., 2001; Vinci et al., 2011).

In these preliminary proof-of concept studies evaluating the skin-liver Chip2, we selected two chemicals with well-described metabolism and modulatory effects on a number of xenobiotic metabolizing enzyme (XME) activities, namely, permethrin and hyperforin. Permethrin is a synthetic pyrethroid used for the treatment of head lice and scabies. Further human exposure can also result from its use as a pesticide. The chemical structure of permethrin and the main metabolic pathway are shown in Fig. 1. The liver is the major site of permethrin metabolism in humans. *In vitro* human metabolism studies showed that CYP3A4 and CYP2C19 are involved in the ester bond cleavage of permethrin (Lavado et al., 2014). However, hCE-1 (human carboxylesterase 1) and hCE-2 are the main enzymes responsible for the hydrolysis of permethrin to 3 phenoxybenzyl alcohol (PBOH, denoted in Fig. 1 as "PM3″) and cis- or trans-3-(2,2 dichlorovinyl)-2,2-dimethyl-(1-cyclopropane) carboxylic acid (CVA, "PM1″) (Hedges et al., 2019). PBOH is subsequently oxidized by alcohol dehydrogenase (ADH) and aldehyde dehydrogenase (ALDH) to phenoxybenzoic acid (PBCOOH, "PM5″) (Choi et al., 2002), and CVA is conjugated to form a glucuronide (Tomalik-Scharte et al., 2005). Hyperforin is a component of St. John's Wort, a popular herb largely used in the treatment of depression but also as a topical remedy for sun protection and as an antimicrobial. It has been implicated in a number of clinically significant interactions with medicinal drugs, including induction of CYP3A4, CYP2E1 and CYP2C19 on the transcriptional level (Moore et al., 2000; Saxena et al., 2008) and competitive and noncompetitive inhibition of several CYP enzymes (*e.g.* CYP2C9, CYP3A4, CYP2D6) (Lee et al., 2006; Obach, 2000; Pal and Mitra, 2006). The chemical structure of hyperforin and the main metabolic pathways are shown in Fig. 2. In *in vitro* studies using human liver microsomes and recombinant CYPs, a total of 57 hyperforin metabolites were detected (Hokkanen et al., 2011). Of those, six were identified as monohydroxides, while the others were formed *via* two or more hydroxylation reactions, *via* dehydrogenation, or by combinations of these reactions. The CYP2C and CYP3A families were shown to play a central role in the metabolism of hyperforin (Hokkanen et al., 2011); therefore, it induces its own metabolism (autoinduction).

The application scenarios were single or repeated doses applied "systemically" to the liver compartment of the Chip2 or topically to the surface of the EpiDerm™ models. The Chip2 experiments were carried out in two laboratories to evaluate the transferability and intra-lab

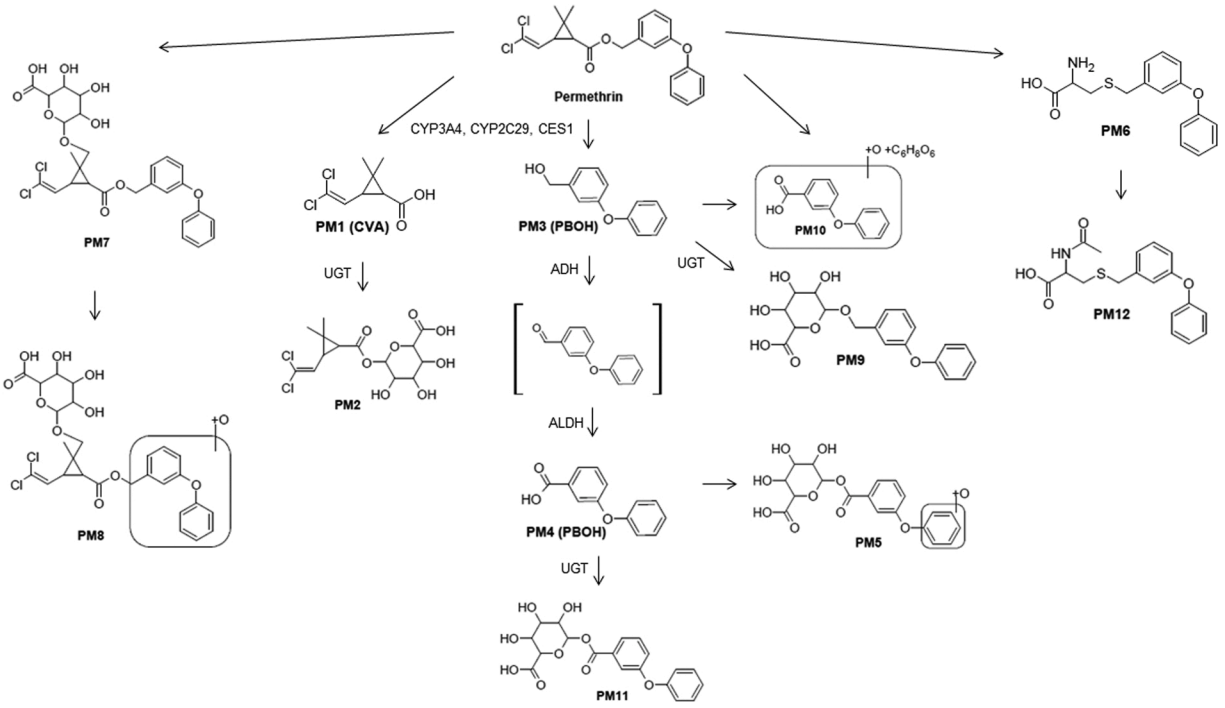

Fig. 1. Permethrin metabolites formed in *in vitro* and *in vivo* and the XMEs involved. ADH = alcohol dehydrogenase, ALDH = aldehyde dehydrogenase; CES1 = carboxylestesterase-1; UGT = UDP-glucuronosyltransferases.

reproducibility of the technology. The maintenance of the viability and metabolic function of the organoids over 6 days in the Chip2 was also assessed.

2. Materials and methods

2.1. Chemicals

Permethrin (Catalogue number 45,614) and hyperforin (dicyclohexylammonium) salt (Catalogue number H1792−1MG) were purchased from Sigma Aldrich. Labs 1 and 2 used the same batches of chemicals. Permethrin was a mixture of cis- and trans-isomers, with 38.7 % *cis*-isomer and 59.4 % *trans*-isomer. The purity was of analytical standard, with the *cis*+*trans*-isomer mix having a purity of 98.1 %. The purity of hyperforin was ≥98 % (measured by HPLC). All other chemicals used in these experiments were of the highest purity.

2.2. Pre-tests using static incubations with either EpiDerm™ models or liver spheroids

Pre-tests were conducted in Lab 2. These static experiments served to determine the effect of permethrin and hyperforin on several parameters in EpiDerm™ models and liver spheroids incubated separately. Measurements included metabolite formation, viability, penetration through the EpiDerm™ models and XME gene expression in liver spheroids. Permethrin was analyzed in a single experiment (n = 3) and hyperforin was analyzed in three separate experiments (n = 3).

2.2.1. Dose selection for static incubations with either EpiDerm models or liver spheroids

Stock solutions of permethrin in DMSO and hyperforin in ethanol were prepared according to the final dose. Both chemicals have a high logP (logP values for permethrin and hyperforin are 7.15 and 8.35, respectively); therefore, aqueous solvents were not suitable for the preparation of stock solutions of test chemicals. While hyperforin was best dissolved in ethanol, we found that DMSO was the better solvent for permethrin in that it tended not to precipitate on the skin surface. The "dose" applied in experiments refers to the final nominal concentration in the medium irrespective of the application volume or route, not including the expected binding to the polydimethylsiloxane (PDMS) circuit or potential binding to the organoid proteins. For systemic application, 4 µl of the stock solution was added to the medium to result in a concentration that was twice as high as the final target concentration. This was then added to an equal volume of medium containing liver spheroids to result in the final concentration. The intended final concentrations of all dosing solutions in culture medium (*via* the systemic route) were confirmed by measuring the concentration in aliquots of 1:1 mix of dosing solution and medium (thus, there was no irreversible non-specific binding to medium proteins). For dermal exposure, 2 µl of the stock solution were applied to the surface of the EpiDerm™. This dose was equivalent to the target concentration in the medium if 100 % of the dose enters the systemic circulation (500 µl).

Concentrations tested in the pre-tests were chosen based on published data. Das et al. (2008) analyzed the effect of 25–200 µM permethrin on human hepatocytes and observed a concentration-dependent induction of CYP3A4 activity and an increased expression of mRNA of multiple CYPs at 100 µM. Minor toxicity of permethrin (according to adenylate kinase release and caspase) was observed at 100 µM but no toxicity was observed at lower concentration (50 µM). Therefore, we tested 1–100 µM permethrin (stock solutions of permethrin from 250 µM to 25 mM). The selection of concentrations for hyperforin was based on studies evaluating its CYP induction effects of concentrations up to ~40 µM. Komoroski et al. (2004) showed a dose-dependent induction in CYP3A4 and CYP2C9 mRNA expression between 0.1 and 1.5 µM (non-pure, unstable form); therefore, we started with a target concentration range of 1–40 µM (stock solutions of hyperforin from 250 µM to 10 mM).

2.2.2. Static incubations with EpiDerm™ models only

EPI-296 epidermis equivalents were purchased from the MatTek Corporation. The 96-well skin models in Millicell hanging inserts were transferred to a 96-well multi-well containing 250 µl EPI-100-NMM-WE medium. EpiDerm™ models were incubated at 37 °C and 5 % CO_2 for 1 h prior to chemical exposure and subsequently incubated, without a

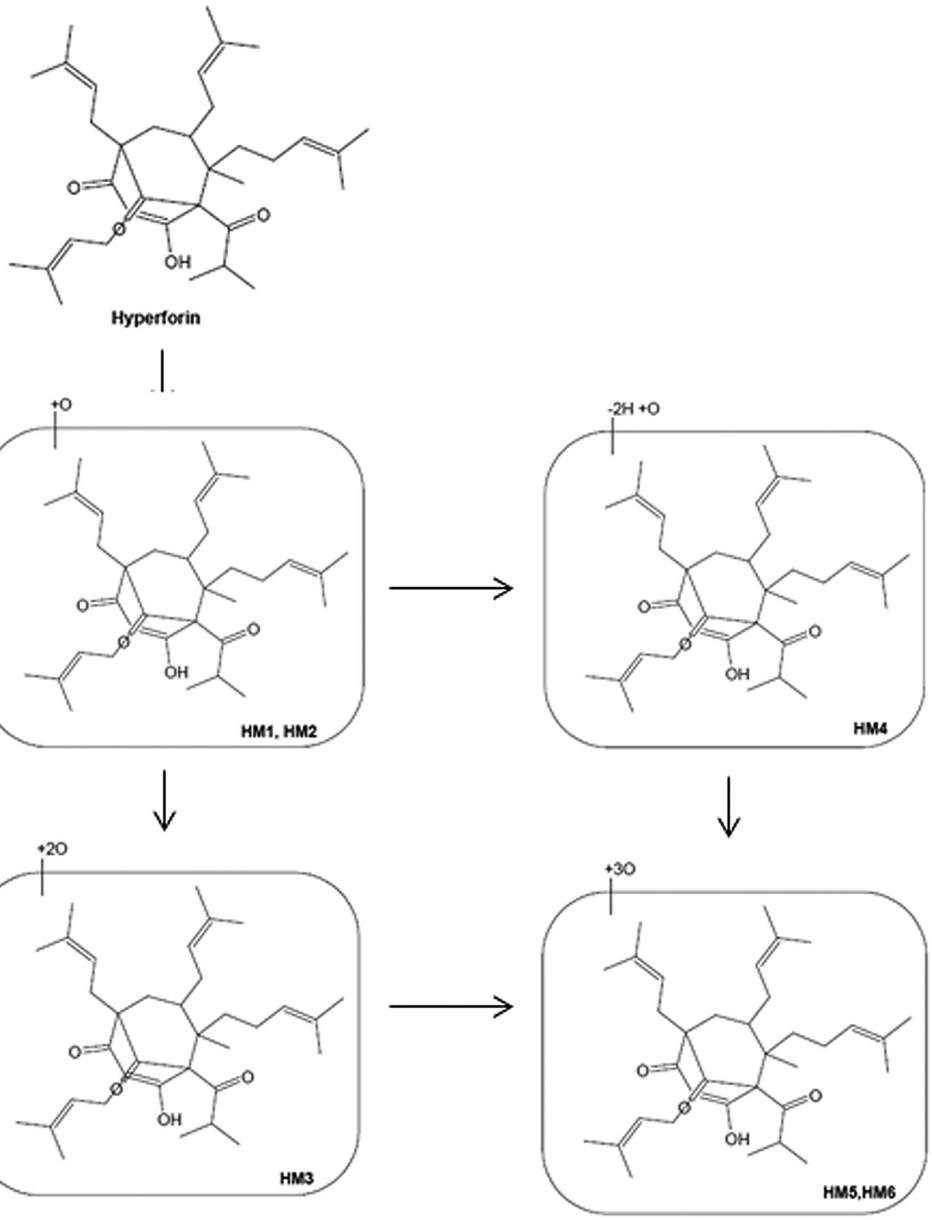

Fig. 2. Hyperforin metabolites formed *in vivo* and *in vitro* according to literature, which were also detected in incubations with liver spheroids in the pre-tests.

medium change, for up to 48 h.

2.2.3. Preparation and static incubation of liver spheroids only

Cryopreserved HHStec were from Provitro (Catalogue number SC-5300) and were cultured in Stellate Cell Medium (SteCM from Provitro) until a confluence of ~80 % was reached. Differentiated HepaRG cells (HPR116) were from Biopredic International (Rennes, France). Four days prior to formation of spheroids, HepaRG cells were thawed and cultured in HepaRG medium containing 0.5 % (v/v) DMSO. The following day, medium was changed to HepaRG medium containing 2% DMSO. HepaRG cells were harvested using trypsin/EDTA and then mixed with HHSteC cells in a 25:1 ratio. This ratio was considered optimal in (a) forming firm spherical spheroids and (b) avoiding fibrotic spheroids, which may occur at a higher ratio of HHSteC cells due to activation, proliferation and extracellular matrix formation. Cells were then pipetted into each well of a 384-well ultra-low attachment plate. Each liver spheroid consisted of 50,000 cells. The fully loaded plate was centrifuged at 100 x g for 1 min and then cultured at 37 °C and 5 % CO_2 on a shaker for 3 days. The spheroids were transferred to 24-well ultra-low attachment plates with 20 spheroids per well in 1 ml. For the incubations, test chemical or its corresponding solvent were added to the appropriate wells. The liver spheroids were then incubated, without a medium change, for 24 and 48 h, at which time points aliquots of the medium were collected for analysis.

2.3. Pre-test to determine non-specific binding in empty Chip2 circuits

In "empty Chip" experiments, chemicals were applied to the Chip2 circuits in exactly the same way as that in the main systemic experiments (see Section 2.4.1), by testing either a single application with daily fresh medium changes or repeated application with medium changes containing the test chemical. Briefly, 250 µl EPI-100-NMM-WE "Co-culture Medium" (from MatTek) was added to the circuit, followed by 250 µl Co-culture Medium containing twice the final concentration of test compound. Final concentrations tested were 5, 25 and 50 µM permethrin and 0.64, 2.5 and 5 µM hyperforin. Subsequent daily medium exchanges were performed by removing 250 µl medium and replacing it with 250 µl fresh medium without test compound (single application) or with test

compound (repeated application). On Day 5, all of the medium was removed from the circuit and 500 µl 100 % DMSO was added. After a further 24 h incubation, all of the DMSO was removed from the circuit. All medium and DMSO samples removed were analyzed for the presence of the parent compound.

2.4. Chip2 experiments with EpiDerm™ and liver spheroids

Skin-liver Chip2 experiments were conducted by two laboratories. "Lab 1″ was TissUse GmbH and "Lab 2″ was Beiersdorf AG. The Chip2 circuits and associated equipment were from TissUse GmbH (Berlin, Deutschland, "Lab 1″). Each application scenario was conducted in one experiment by both laboratories, with n = 5 Chip2 circuits tested in Lab 1 and n = 3 circuits tested in Lab 2. The same batches of EpiDerm™ models, HepaRG cells and HHStec were used in both laboratories by the same personnel.

2.4.1. Set up of the skin-liver Chip2 and application of chemicals

The Chip2 circuits were filled with EPI-100-NMM-WE "Co-culture Medium" at least one day prior to the start of the Chip2 experiment. Twenty liver spheroids (prepared as described in Section 2.2.3) were transferred to the spheroid culture compartment of the Chip2, and EpiDerm™ trans-well inserts were integrated into the second culture compartment. The Chip2 experiments employed the same 96-well EPI-296 epidermis equivalents in Millicell hanging inserts as those used in the static experiments. A volume of 500 µl medium was added to the circuit and subsequent daily medium exchanges were performed by removing 250 µl and replacing it with 250 µl fresh medium. The Chip2 circuits were connected to the HUMIMIC Starters operating unit at a pressure of 350 mbar and vacuum of 300 mBar with 0.5 Hz as the pump frequency, resulting in a flow rate of 2.7 (± 0.2) µl/min.

The target doses for permethrin and hyperforin were 25 and 1.25 µM, respectively. For comparative assessment of exposure route effects, the chemical was either applied to the surface of the EpiDerm™ model (2 µl per model, topical) or to the liver compartment of the Chip2 (systemic). A single dose scenario refers to the application of the chemical at "Day 0″ (*i.e.* 24 h after the EpiDerm™ models and liver spheroids had been added to the Chip2 compartment). A repeated dose scenario refers to the application of chemical on Day 0 and reapplication (without washing the skin surface) every 24 h after this time point (*i.e.* Day 1, 2, 3 and 4). The "dose" refers to the final concentration in the whole systemic circulation irrespective of the application volume or route. For example, the target "dose" of permethrin was 25 µM, which was the expected medium concentration after application of 2 µl of a 6250 µM stock solution in DMSO to the skin surface and 100 % entering the 500 µl circuit volume. For systemic application, the dose was added during the "half medium change" (the removal of 250 µl from the circuit and addition of 250 µl fresh medium) – therefore, 250 µl medium containing twice the final concentration was added to the circuit after 250 µl of the "old medium" was removed.

2.4.2. Medium sampling from the Chip2 circuit

At early time points up to 8 h, 80 µl of the circuit medium was removed and transferred to an Eppendorf tube. On Day 1–5, 250 µl of the 500 µl circuit medium was removed and, of this, 80 µl was aliquoted into Eppendorf tubes or 96-well plates for MS analysis and stored at −80 °C. All remaining supernatants were transferred into 96-deep well plates and stored at 4 °C until LDH, glucose, lactate and albumin analyses were performed. At the end of the culture period, tissues were harvested from the Chip2 and processed further for histochemical and qPCR analysis.

2.4.3. Tissue harvest from the Chip2 circuit

To analyze the tissues at different time points (Day 1, Day 2 and Day 5) of exposure, respective Chip2 experiments were stopped and EpiDerm™ models and liver spheroids were collected and subjected to histological and transcriptional analyses. Several liver spheroids were transferred to a cryomold filled with TissueTek and frozen at −80 °C. EpiDerm™ models were cut in half. One half was transferred into a cryomold with TissueTek and frozen at −80 °C. For cryosectioning, both tissues were transferred to the cryostat and sectioned at a blade temperature of −18 °C and object head temperature of −17 °C. After reaching the central region, sections with an 8 µm thickness were cut and transferred to object slides. The glass slides were stored at room temperature for drying and subsequently stored at −20 °C until hematoxylin & eosin (H&E) staining. The other half of the EpiDerm™ model and the rest of liver spheroids were transferred into "RA1 lysis buffer" (from the NucleoSpin 8 RNA Core Kit (Macherey Nagel, REF 740465.4)) for mRNA expression analysis. These samples were frozen and stored at −80 °C until RNA isolation.

2.5. End point measurements employed in static and Chip2 experiments

2.5.1. Viability measurements

The viability of the organoids in static and Chip2 experiments was measured using several end point parameters. A decrease in the value of the viability end point of more than 10 % of the solvent control value was considered to be a biologically relevant loss of viability. End points included the following: MTT (3-(4,5-dimethylthiazol-2-yl)-2,5-diphenyltetrazolium bromide) metabolism (static EpiDerm™ models only), ATP content (static liver spheroids only), albumin production (static liver spheroids and Chip2 experiments), glucose consumption (Chip2 experiments only), lactate production (Chip2 experiments only), and release of LDH (static incubations with EpiDerm™ models and liver spheroids, and Chip2 experiments). The structure of EpiDerm™ models was also monitored using H&E staining and immunohistochemical staining of nuclei (DAPI, blue), proliferation marker (Ki67, red) and apoptosis marker (TUNEL, green).

For the MTT assay, EpiDerm™ models were incubated with MTT in NMM-WE medium for 3 h before extraction of the metabolite with isopropanol and measurement of the absorbance at 590 nm. ATP was measured using the CellTiter-Glo 3D assay from Promega (Catalogue number G9682).

Human serum albumin content of the medium was measured in Lab 1 using Albumin in Urine / CSF FS Kit from DiaSys and in Lab 2 using the "Human Albumin ELISA Quantitation Set" from Bethyl Laboratories, Inc. (Catalogue number E80−129).

Lactate concentrations in the medium were measured in Lab 1 using the FluitestR Lactate kit from Analyticon and in Lab 2 using the "lactate determination kit" from Diaglobal GmbH (Catalogue number LAC 142). Glucose concentrations in the medium were measured in Lab 1 using the Glucose (HK) Kit (Catalogue number 981,779) from Thermo Fisher Diagnostics and in Lab 2 using the "glucose determination kit" from Diaglobal GmbH (Catalogue number GLU 142).

The LDH content of the medium and lysed EpiDerm™ models and liver spheroids was measured in Lab 1 using the LDH (IFCC) Kit from Thermo Fisher Diagnostics and in Lab 2 using the "Cytotoxicity Detection KitPLUS (LDH) from Roche. Concentrations were quantified using an LDH standard from Roche (L-LDH, 10,127 230 001) to construct a calibration curve from 0.781 to 50 mU/ml. The viability in static and Chip2 experiments was calculated as a percentage of the LDH in the medium compared to the total LDH content in the incubation *i.e.* one EpiDerm™ model and/or 20 liver spheroids.

The total LDH content each EpiDerm™ model and 20 liver spheroids was determined by releasing all LDH using a lysis method. This was achieved by incubating them separately for 1 h in 500 µl 0.1 % Triton X-100, followed by homogenization using a tissue shredder. The samples were centrifuged before taking an aliquot for LDH analysis. For static incubations with a single organoid, the total LDH for that organoid was used to calculate viability; whereas, for Chip2 experiments, the total LDH content was the sum of the LDH in one EpiDerm™ model and 20 liver spheroids. The following calculations were used to calculate relative viability in static and Chip2 experiments.

$$\text{Adjusted LDH activity } (LDH_{MED,ADJ}) = LDH_{MED} - LDH_{BLANK} \quad (1)$$

Where the LDH activity in medium sample = LDH_{MED} and LDH activity in blank (fresh medium without any organoids) = LDH_{BLANK}

$$\%\ Viability\ of\ organoids = \frac{LDH_{TOTAL} - LDH_{MED,ADJ}}{LDH_{TOTAL}} \times 100 \quad (2)$$

Where LDH_{TOTAL} represents the LDH activity in lysed organoid(s) (Total LDH).

The viability of the organoids after application of test chemical was expressed as a percentage of the viability of the solvent control treated Chip2:

$$\%\ \text{of solvent control viability} = \frac{\%\text{viability after chemical application}}{\%\text{viability solvent application}} \times 100 \quad (3)$$

The integrity of the EpiDerm™ models was assessed according to TEER values measured within the 96-well Millicell inserts using a 3D-printed trans-well-mount. This device was developed by TissUse GmbH (Lab 1) for the Chip2 to ensure reproducible TEER values. The TEER measurements were in accordance with the expected TEER values measured in standard Trans-wells (data not shown).

2.5.2. qPCR analysis of liver spheroids

The isolation of total RNA from the liver spheroids was performed using the NucleoSpin® RNA Kit (Lab 1) or the RNeasy® Mini Kit from Qiagen (Lab 2). After collection, tissues were directly re-suspended in lysis buffer, containing the reducing agent β-mercaptoethanol and stored at −80 °C until further processing. After thawing the samples, the RNA-isolation was performed following the manufacturer's instructions. The RNA was finally eluted in RNase-free H_2O. The concentration and purity of the isolated RNA was determined using a NanoDrop spectrophotometer. The RNA was either used immediately for cDNA synthesis, or stored at −80 °C. cDNA synthesis by reverse transcription was carried out with the TaqMan® Reverse Transcription Reagents (Lab 1) or Applied Biosciences High Capacity cDNA Reverse Transcription Kit (Lab 2).

Real-time qPCR analysis of permethrin and hyperforin samples was performed in Lab 1 using the SensiFAST™ SYBR® Lo-ROX kit. Every PCR reaction contained 7.5 µl cDNA and 2.5 µl primer mix and was analyzed with the QuantStudio® 5 Real-Time PCR System. At Lab 2, Real-time qPCR for the permethrin samples was carried out using TaqMan® Low Density Arrays (LDA), according to the manufacturers' instructions. Real-time qPCR analysis of hyperforin samples was performed using the RT^2 SYBR Green ROX qPCR Mastermix and Custom RT^2 Profiler PCR Arrays (Format E) from Qiagen, according to the manufacturers' instructions. The expression-levels were quantified through normalizing the cycle thresholds (as the measured values) of the genes of interest to a housekeeping gene, according to the following formula with E = amplification efficiency, HK = housekeeping gene, target = gene of interest:

$$\frac{E_{target}^{ct}}{E_{HK}^{ct}}$$

Genes measured were: XME genes: CYP1A1, CYP1A2[h], CYP2A6, CYP2B6, CYP2C9, CYP2C19, CYP3A4, CYP3A5 [h], CYP2E1[h], ALDH1A1, ADH1A[p], AKR1C1[p], EPHX1, HCE1 (CES1), HCE2 (CES2), GSTP1[h], GSTM1, SULT1A1[h], SULT1E1[h] UGT1A1, UGT1A9, PTGS2[h], BAAT [h]; transporter genes included: ABCB1 (MDR1), ABCC3 (MRP3)[p], ABCC4 (MRP4)[p]; functional genes included: albumin, caspase-3, Ki67[p], AK1[p], RNGTT, MMP9, PSMC3; and house−keeping genes included: TBP, GAPDH. Genes with a superscript "p" or "h" were tested in permethrin or hyperforin incubations only, respectively.

2.5.3. Parent and metabolite analysis

Medium samples for Liquid Chromatography - Tandem Mass Spectrometry (LC–MS-MS) metabolite analysis were prepared by adding 40 µl acetonitrile plus internal standards (griseofulvin, diazepam and diclofenac) to 40 µl of the standards or samples, respectively. After centrifugation (2200 x g, 5 min at room temperature), the supernatant was transferred into vials for quantification of permethrin, hyperforin and semi-quantitative measurement of their metabolites. The HPLC system consisted of a Dionex UltiMate 3000 RS pump and Dionex UltiMate 3000 RS column compartment and Accela Open Autosampler (Thermo Fisher Scientific, USA).

For permethrin samples, LC was performed in the gradient mode using 0.1 % formic acid in acetonitrile (solvent A) and 0.1 % formic acid in water (solvent B); the pump flow rate was set to 600 µl/min. Separation was performed on an Accucore Phenyl-Hexyl, 2.6 µm, 50 × 2.1 mm (Thermo Fisher, Germany) analytical column with a pre-column C6-Phenyl, 2.6 µm, 4 × 2.0 mm (Thermo Fisher, Germany) for quantification using gradient elution. The gradient was: 0.0 min = 5 % A; 0.1 min = 5 % A; 1.6 min = 97 % A; 2.7 min = 97 % A; 2.8 min = 5 % A and 3.5 min = 5 % A. The sample injection volume was 12 µl. The LLOQ (lower limit of quantification) for permethrin was 15.6 nM. Permethrin was confirmed to be soluble in medium up to 500 µM.

For hyperforin, LC was performed in the gradient mode using acetonitrile (solvent A) and 10 mM ammonium acetate in water (solvent B); the pump flow rate was set to 600 µl/min. Separation was performed on an Kinetex Phenyl-Hexyl, 2.6 µm, 50 × 2.1 mm (Phenomenex, Germany) analytical column with a pre-column C6-Phenyl, 2.6 µm, 4 × 2.0 mm (Thermo Fisher, Germany) for quantification gradient elution. The gradient was: 0.0 min = 5 % A; 0.1 min = 5 % A; 1.4 min = 97 % A; 2.7 min = 97 % A; 2.8 min = 5 % A and 3.5 min = 5 % A. The sample injection volume was 1 µl. The specified LLOQ hyperforin was 1 nM. Hyperforin was confirmed to be soluble in medium up to 40 µM.

Mass spectrometry (MS) was performed on a Q-Exactive Plus mass spectrometer (Orbitrap™ technology with accurate mass) equipped with an H-ESI (heated electrospray interface) (Thermo Fisher Scientific, USA) connected to a PC running the standard software Xcalibur 4.0.27.19. The most abundant and structure characteristics of permethrin and hyperforin metabolites observed and assigned by accurate mass spectroscopic analysis are shown in Supplementary Table 1. A complete metabolite FullScan (in the negative and positive for permethrin and in the negative only for hyperforin) electrospray ionization modes with high resolution (70,000) analysis of the samples was performed to identify metabolic species by accurate mass. Blank samples were the respective medium without test chemical or organoids. Where applicable, MS/HRMS spectra were taken for structural elucidation. For permethrin, the MS was operated in the full scan MS-selected ion monitoring (MS-SIM) (*m/z*: 120–800) mode. The *m/z* value for the [M+H]+ and [M−H]- ion of permethrin was 391.0862 and 389.0706, respectively. For hyperforin, the MS was operated in the full scan MS-SIM (*m/z*: 120–900) mode. The *m/z* value for the [M−H]- ion of hyperforin was 535.3780. The putative metabolites were identified based on the test item fragmentation pattern of the precursor compound and their corresponding characteristic fragments, as shown for permethrin and hyperforin in Supplementary Table 1.

An indication of the metabolic functionality of the organoids over time was determined by calculating the increases in metabolite concentrations over 24 h *i.e.* the time between the half-medium changes. In the absence of standards for quantification, peak areas were used for estimating relative changes in metabolite concentrations. The concentration of metabolites in the circuit directly after medium change was halved due to the removal of half the medium and the addition of 250 µl fresh medium (the "half-medium change"). This new diluted concentration of total metabolites ($Conc_{med\ 1}$) was not actually measured but can be calculated by dividing the measured concentration at that time point by 2:

Table 1
Overview of pre-test results using static organoid incubations over 48 h. Permethrin was tested at 1 – 100 μM and hyperforin was tested at 0.004 – 40 μM in both EpiDerm™ models and liver spheroids. When the loss of viability compared to the solvent control-treated incubations was less than 10 %, the chemical was considered "not cytotoxic". Cytotoxic concentrations of chemical caused more than 10 % loss of viability compared to solvent control-treated incubations. NA = not applicable, ND = not determined.

Parameter	Permethrin		Hyperforin	
Non-specific binding in circuits without EpiDerm™ or liver organoids	Extensive binding (94−96 % adsorbed) in 24 h - ~60 % recovered by DMSO wash		Extensive binding (75−85 % adsorbed) in 24 h and 4−9 % recovered by DMSO wash	
	EpiDerm™	Liver spheroids	EpiDerm™	Liver spheroids
Cytotoxicity – MTT metabolism	Not cytotoxic over 1–100 μM	ND	Not cytotoxic over 0.004–40 μM.	ND
Cytotoxicity – ATP content	ND	Not cytotoxic over 1–100 μM	ND	Tested 0.004–40 μM. Cytotoxic at $\geq$ 0.32 μM at 24 and 48 h.
Cytotoxicity – Albumin production	ND	Not cytotoxic over 1–100 μM	ND	Tested 0.004–40 μM. Cytotoxicity evident at $\geq$ 0.32 μM at 24 and 48 h.
Cytotoxicity – LDH	Not cytotoxic over 1–100 μM	Not cytotoxic over 1–100 μM	Not cytotoxic over 0.004–40 μM.	Tested 0.004–40 μM. Cytotoxicity evident at $\geq$ 5 μM at 24 and 48 h.
Penetration through EpiDerm™ organoids	Very low at all doses tested (1–100 μM) – only trace amounts of parent in medium over 48 h.	NA	Increasing penetration with increasing dose (1−20 μM) – 17 %, 2.8 % and 0.1 % of the applied dose of 1, 5 and 20 μM parent after 24 h	NA
Metabolites produced	No metabolites detected in the medium	12 confirmed metabolites including major *in vivo* metabolites: CVA and its conjugates, PBOH and PBCOOH	2 single and 1 double oxidized metabolite detected	6 metabolites identified, including all major metabolites reported *in vitro* were also produced in liver organoids
XME, transporter or functional gene induction	ND	Majority of genes not altered and genes that were affected (UGT1A1, CYP2B6, CYP1A1) were induced by less than 3-fold	ND	Main effect on CYP3A4 (42-fold induction), with minor induction of: CYP1A1, CYP2B6, and CYP3A5 induced by up to 3-, 2- and 2.1-fold, respectively
Precipitation on skin surface	Precipitation evident – starting at 25 μM after 48 h	NA	No precipitation	NA

Table 2
Effect of systemic and topical application of solvents and test chemicals on TEER values of EpiDerm™ models in the Chip2 circuits over 6 days. Values are expressed as Ω/cm^2 and are taken from one lab (Lab 1) and are a mean ± SD. ns = not statistically significant ($P < 0.05$) from the corresponding solvent control (SC) measurement at the same time point.

	TEER values (Ω/cm2) on Treatment day			
	−1 (n = 42)	0 (n = 6)	2 (n = 3)	5 (n = 3)
Systemic application				
No application	501 ± 172	649 ± 93	ND	578 ± 105
SC for permethrin – single			651 ± 120	549 ± 135
SC for permethrin - repeated			583 ± 93	537 ± 42
Permethrin – single			646 ± 28 (ns)	700 ± 77 (ns)
Permethrin - repeated			671 ± 64 (ns)	712 ± 80 (ns)
SC for hyperforin – single			544 ± 5	452 ± 62
SC for hyperforin - repeated			452 ± 62	454 ± 65
Hyperforin – single			515 ± 129 (ns)	537 ± 47 (ns)
Hyperforin - repeated			474 ± 37 (ns)	545 ± 121 (ns)
Topical application				
No application	495 ± 160	514 ± 126	ND	502 ± 30
SC for permethrin – single			390 ± 26	398 ± 20
SC for permethrin - repeated			381 ± 42	356 ± 86
Permethrin – single			387 ± 5 (ns)	494 ± 47 (ns)
Permethrin - repeated			453 ± 25 (ns)	387 ± 61 (ns)
SC for hyperforin – single			416 ± 46	432 ± 65
SC for hyperforin - repeated			323 ± 22	189 ± 36
Hyperforin – single			417 ± 60 (ns)	584 ± 123 (ns)
Hyperforin - repeated			323 ± 46 (ns)	245 ± 18 (ns)

$$\text{Total metabolite concentration after half-medium change } (\text{Conc}_{\text{med 1}}) = \frac{\sum \text{peak areas in medium}}{2}$$

Metabolites continue to be formed over the following 24 h and are directly measured in the subsequent sample of medium removed from the circuit. The total concentration of total metabolites in this sample was calculated to be:

Metabolite concentration at the subsequent medium change $(\text{Conc}_{\text{med 2}}) = \sum$peak areas in medium

Therefore, the difference between the time points over 24 h was equivalent to the activity:

$$\text{Activity(peak area increase/h)} = \frac{\text{Conc}_{\text{med 2}} - \text{Conc}_{\text{med 1}}}{24\ \text{h}}$$

The main permethrin metabolites (according to peak area) were assigned as PM1, PM2, PM3, PM5, PM6, PM9, PM11 and PM12 and the main hyperforin metabolites were assigned as HM1, HM2, HM3 and HM6.

2.6. Statistical analysis

All experiments were carried out with more than three independent experimental setups. Values are expressed as a mean ± SD. Statistical analyses were conducted using Prism GraphPad software, Version 8.4.3. Statistical differences for fold induction of genes were conducted by first transforming fold-induction values into log2[fold-induction], and then testing with a one-sample *t*-test whether the mean was significantly different from 0 (for this, a statistical difference is denoted with * when $p < 0.05$). All other statistical differences were evaluated using unpaired two-tailed *t*-test for analysis of two samples and one-way ANOVA with Greisser-Greenhouse correction and Dunnett post-hoc test for multiple comparison of matched data with one variable and two-way ANOVA with Greisser-Greenhouse correction and Turkeys post-hoc test for matched data with two variables. A statistical difference is denoted with * when $p < 0.05$, with ** when $p < 0.01$ and *** when $p < 0.001$ (Table 1).

3. Results

3.1. Single static incubation with EpiDerm™ or liver spheroids for selection of the test doses

A range of doses of each test chemical was evaluated in separate static incubations of EpiDerm™ models and liver spheroids for 24 and 48 h to determine the optimal dose for the Chip2 experiments. Applied criteria for the final dose were that the chemical (1) was metabolized at least by liver spheroids, (2) showed some penetration of the EpiDerm™ models, (3) was non-cytotoxic and, (4) ideally, altered XME gene expression in the liver spheroids as indication for their responsiveness to chemical exposure. An overview of the results from the static incubations with EpiDerm™ models and liver spheroids is shown in Table 2.

3.1.1. Organoid viability

The viability of the EpiDerm™ models was assessed by measuring their metabolism of MTT, as well as LDH leakage into the medium. Both cytotoxicity markers confirmed that neither chemical was toxic to EpiDerm™ models at any of the doses tested. The viability of liver spheroids was assessed based on three endpoint parameters, namely, ATP content, human serum albumin production and LDH leakage. Permethrin was not toxic to liver spheroids at 24 or 48 h at any of the concentrations tested (1–100 μM). In contrast to permethrin, hyperforin was very toxic to the liver spheroids, whereby, in the first experiment, it was markedly toxic at most concentrations tested (1–40 μM). Additional experiments tested much lower concentration ranges, starting with 0.004 μM to a maximum of 1 μM. A decrease in albumin production was the most sensitive indicator of cytotoxicity, since this was decreased at concentrations which did not affect ATP content and LDH release. Based on albumin production, 0.16 μM was the highest non-cytotoxic hyperforin concentration and at the next higher dose, 0.32 μM, albumin production decreased to 67 % of solvent control-treated organoids. At 0.32 μM ATP was also decreased to 66 % after 24 h, whereas LDH release increased only after 48 h at 5 μM and higher.

3.1.2. Penetration through EpiDerm™ models

The penetration of different doses of chemicals through EpiDerm™ models in static incubations was measured over 48 h. Only minimal penetration of permethrin through the EpiDerm™ models was observed. After application of doses of 5–100 μM, only trace amounts (<50 nM) of permethrin were sometimes detected in the medium, which were neither dose- nor time dependent. At 25 μM, only 0.06 % of the applied dose reached the medium below the EpiDerm™ models by 48 h. In contrast to permethrin, all doses of hyperforin between 0.64 and 5 μM slowly penetrated the EpiDerm™ models (~2 % and 1–3 % of the applied dose by 24 h and 48 h, respectively), with a lag time of at least 6 h of the parent chemical (hyperforin was only present in the medium at the 12 h time point).

3.1.3. Metabolism in EpiDerm™ models and liver spheroids

Permethrin was extensively metabolized by liver spheroids, whereby

more than 90 % was depleted by 24 h. Twelve metabolites were identified, including all of the main *in vivo* metabolites denoted in Fig. 1. Hyperforin was more slowly metabolized by liver spheroids, in which 40–60 % of the initial amount remained after 24 h and 31–49 % after 48 h. Ten oxidized metabolites of hyperforin were produced in liver spheroid incubations (Fig. 2), including the main single (HM1 and HM2) and double oxidized products detected *in vivo* (HM5 and HM10).

No permethrin metabolites were detected in the media of EpiDerm™ model following topical application (parent and metabolites in the EpiDerm™ models were not determined). By contrast, six oxidized metabolites of hyperforin were produced as it passed through the EpiDerm™ models. These included HM1, HM2, HM3 and HM4, which are single oxidation metabolites, HM5, which is a double oxidation metabolite and HM6, which is formed *via* hydration and oxidation. The formation of these metabolites indicates that the EpiDerm™ models had functional CYP activities.

It was not possible to quantify any of the metabolites due the lack of reference material; therefore, for simplicity of presentation in this paper, we have only reported on findings on the metabolites known to be produced *in vivo* and with the highest peak areas (although it is acknowledged that peak areas are only semi-quantitative).

3.1.4. Liver spheroid XME gene expression

The majority of the 22 XME, transporter and functional genes measured in liver spheroids were not altered by permethrin compared to solvent control and genes that were affected were induced by less than 3-fold. While CYP3A4 was not markedly or dose-dependently induced in liver spheroids, another PXR-regulated gene that was induced in a dose-dependent manner was UGT1A1 (fold increases by 5, 25 and 50 μM permethrin were 1.2 ± 0.5 (not significant), 1.9 ± 0.2 ($p < 0.05$) and 2.6 ± 0.4 ($p < 0.05$), respectively after 24 h). CYP2B6 was also induced by approximately 2-fold but this was not dose-dependent (fold increases by 5, 25 and 50 μM permethrin were 1.1 ± 0.1 (not significant), 1.8 ± 0.5 (not significant) and 1.9 ± 0.2 ($p < 0.05$), respectively after 24 h and 1.8 ± 0.6 (not significant), 2.0 ± 0.2 ($p < 0.05$) and 1.9 ± 0.3 ($p < 0.05$), respectively after 48 h). The AhR-regulated gene, CYP1A1, was induced in a dose-dependent manner (fold induction after 24 h by 5, 25 and 50 μM permethrin was 1.2 ± 0.5 (not significant), 1.9 ± 0.1 (not significant) and 2.8 ± 0.6 ($p < 0.05$), respectively).

The levels of 27 XME, transporter and functional genes were measured in liver spheroids treated with hyperforin. This chemical at concentrations of 0.64 and 1 μM induced several genes after 24 h and 48 h. These concentrations may have caused some toxicity, but they were not overtly toxic based on the LDH leakage measurements and the fact that XME genes were induced, as this would not happen if the organoids were completely compromised. The highest fold induction was observed with CYP3A4, which was statistically significantly ($p < 0.05$) induced by 0.64 and 1 μM hyperforin by 32.5 ± 12.4-fold and 15.6 ± 12.6-fold after 24 h by, respectively, and by 17.5 ± 6.1 and 48.0 ± 49.9-fold after 48 h, respectively. There was also a small but statistically significant ($p < 0.05$) induction by 0.64 and 1 μM hyperforin of CYP1A1 at 48 h (2.1 ± 1.9-fold and 2.9 ± 1.6-fold, respectively), CYP2B6 at 24 h (3.2 ± 1.5-fold and 2.1 ± 1.1-fold, respectively), and CYP3A5 at 24 h (2.8 ± 0.8-fold and 2.2 ± 0.5-fold, respectively).

3.1.5. Non-specific binding

The selection of the optimal dose for the Chip2 experiments also depends on the non-specific binding of the chemical to the organoid compartment and circuit walls. A marked decrease in the free fraction of a chemical due to this effect would affect the ability to detect it and its metabolites, as well as reduce any impact the chemical has on organoid XMEs. In the absence of protein (*i.e.* an empty chip), permethrin bound to the walls of the Chip2 circuit during the first 24 h (4–6 % of the initial

Table 3
Comparison of conditions used for static and dynamic incubations. The values stated for the % binding of different doses of permethrin and hyperforin in the Chip2 model are shown together with the mean (± SD) measured concentrations in the circuit on Day 2, 3 4 and 5 (in parentheses) during which time the concentrations had reached a plateau.

	Static	Dynamic
EpiDerm model used	EPI-296 epidermis equivalents 96-well skin models in Millicell hanging inserts	
Medium	EPI-100-NMM-WE medium (recipe proprietary but known to contain BSA)	
Volume	250 μl	500 μl
% binding in the absence of EpiDerm™ or liver spheroids	Hyperforin: 17 % (3 h) Permethrin: 47 % (3 h)	Hyperforin: 0.64 μM = 82 % (0.115 ± 38 μM) 2.5 μM = 35 % (1.61 ± 0.23 μM) 5 μM = 38 % (3.12 ± 0.66 μM) Permethrin: 5 μM = 99 % (0.101 ± 0.03 μM) 25 μM = 93 % (0.70 ± 0.39 μM) 50 μM = 85 % (1.5 ± 0.81 μM)
% binding in the presence of heat-inactivated liver spheroids	Hyperforin: 16 % (3 h) Permethrin: 0 % (3 h)	Not measured
Occlusion	Partial-occlusion: covered with a standard plate lid, allowing for some evaporation	Complete occlusion: compartment closed with a screw lid

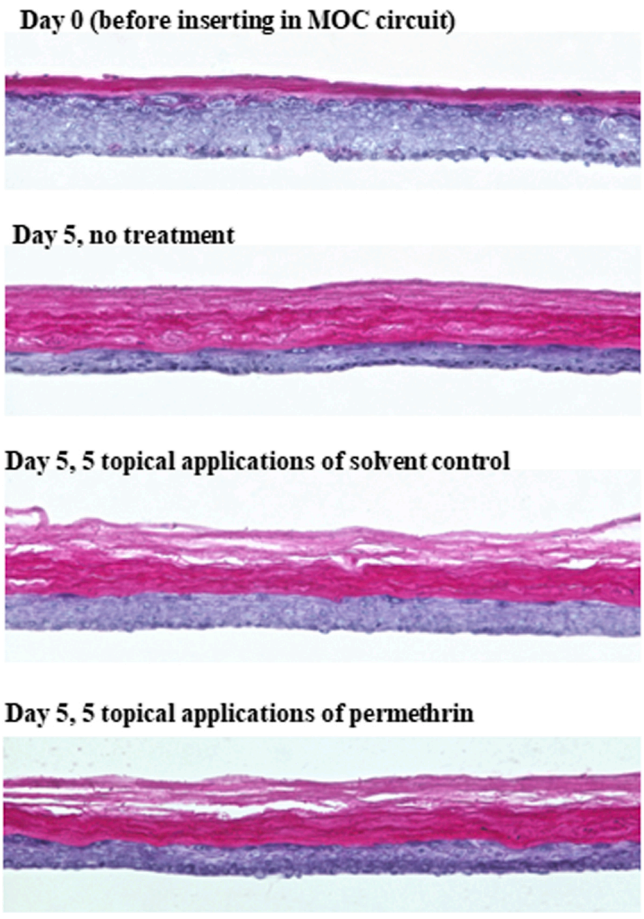

Fig. 3. H&E staining of cross-sections of EpiDerm™ over time and with application of solvent or permethrin.

concentration remained). This binding was readily reversible using medium or DMSO washes.

Hyperforin also bound to the walls of the Chip2 circuit during the first 24 h, although the extent of loss of parent chemical (35 %–82 % of the initial concentration remained after 24 h) was less than for permethrin, with saturation of binding occurring at a concentration between 0.64 and 2.5 μM (Table 3). Since liver spheroid pre-tests showed that concentrations higher than 0.32 μM caused a decrease in liver spheroid functionality (albumin production and ATP content), the concentration of hyperforin in empty chip experiments after systemic application was used to estimate the highest safe dose that would be expected to induce XMEs. The repeated application of 0.64 μM and 2.5 μM hyperforin to empty chips over 5 days resulted in maximum concentrations measured in the medium of 115 nM and 1.6 μM, respectively. Unlike permethrin, the presence of protein (*i.e.* heat-inactivated liver spheroids) did not markedly alter the extent of non-specific binding in polycarbonate plates (Table 3); therefore, empty chip concentrations were taken to represent levels that would be present in Chip2 circuits containing organoids. We considered 115 nM to be too low (it may not cause changes to the XMEs and metabolites may not be measurable) and 1.6 μM to be too high (causing toxicity). Therefore, we set the nominal target test dose of hyperforin for the Chip2 experiments at 1.25 μM. This equates to 0.23−0.81 μM once non-specific binding in PDMS circuits (35–82 %, Table 3) was considered. Although this range overlaps the concentration at which cytotoxicity started to be evident in the static experiments with liver spheroids (0.32 μM), it is also in the range of concentrations shown to result in a good induction of CYP3A4 (0.64 and 1 μM). It was assumed that the susceptibility of liver spheroids to toxicity would be lower in the Chip2 because of the dynamic flow of medium, the controlled oxygenation of the medium and the daily half medium changes. This was supported by the viability data from the Chip2 experiments (see Section 3.2.2).

3.1.6. Chemical precipitation

The appearance of the EpiDerm™ models was monitored after topical application of the chemicals. While neither vehicle nor hyperforin affected the appearance of the surface of the EpiDerm™ models, permethrin appeared to precipitate. The effect was apparent, although minimal, at 25 μM and increased with increasing doses. For this reason, we considered 25 μM to be the likely optimal target nominal dose for permethrin since this was the highest concentration with minimal precipitation. The observations of permethrin in these tests were made on partially occluded EpiDerm™ models (a plate lid was applied), and the same degree of precipitation was not expected in the Chip2 because it was completely occluded and the surface was moist.

3.2. Chip2 experiments – viability measurements

3.2.1. EpiDerm™ H&E histology and TEER values

There was a good maintenance of the EpiDerm™ structure over 5 days after systemic and topical application of solvents or test chemicals. An example of the H&E staining of sections of EpiDerm™ models taken from experiments in Lab 1 with the repeated topical application of DMSO or permethrin is shown in Fig. 3 (treatment with hyperforin not shown). This treatment can be considered to be the most mechanically disruptive handling compared to systemic application, since the solvent or chemical was directly applied to the EpiDerm™ surface. Topical application of solvents or test chemicals resulted in very minor disruption of the stratum corneum (which became thicker over time) and an intact epidermis up to Day 5. This finding was in accordance with the

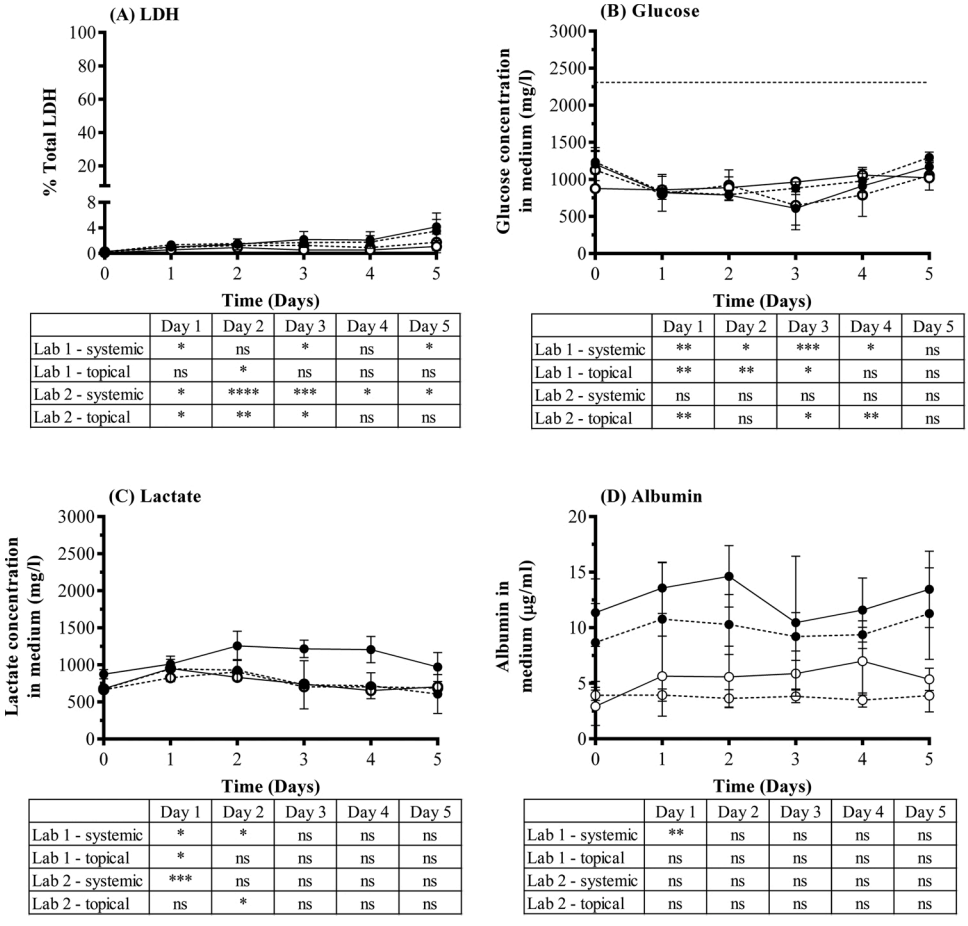

(A) LDH	Day 1	Day 2	Day 3	Day 4	Day 5
Lab 1 - systemic	*	ns	*	ns	*
Lab 1 - topical	ns	*	ns	ns	ns
Lab 2 - systemic	*	****	***	*	*
Lab 2 - topical	*	**	*	ns	ns

(B) Glucose	Day 1	Day 2	Day 3	Day 4	Day 5
Lab 1 - systemic	**	*	***	*	ns
Lab 1 - topical	**	**	*	ns	ns
Lab 2 - systemic	ns	ns	ns	ns	ns
Lab 2 - topical	**	ns	*	**	ns

(C) Lactate	Day 1	Day 2	Day 3	Day 4	Day 5
Lab 1 - systemic	*	*	ns	ns	ns
Lab 1 - topical	*	ns	ns	ns	ns
Lab 2 - systemic	***	ns	ns	ns	ns
Lab 2 - topical	ns	*	ns	ns	ns

(D) Albumin	Day 1	Day 2	Day 3	Day 4	Day 5
Lab 1 - systemic	**	ns	ns	ns	ns
Lab 1 - topical	ns	ns	ns	ns	ns
Lab 2 - systemic	ns	ns	ns	ns	ns
Lab 2 - topical	ns	ns	ns	ns	ns

Fig. 4. Organoid viability in the Chip2 circuit according to (A) LDH leakage, (B) glucose, (C) lactate and (D) albumin contents in the medium over time after repeated systemic and topical application of the solvent controls. Values in experiments in Lab 1 (closed circles, n = 6) and Lab 2 (open circles, n = 4-5) are a mean ± SD. Values with a dotted line represent topical application and values with a continuous line represent systemic application. In (C), the dotted line at the 2300 mg/l value represents the concentration of glucose in fresh medium. The % viability of organoids was calculated according to Eq. 2. A statistical difference from the Day 0 medium measurement is denoted with * when $p < 0.05$, with ** when $p < 0.01$ and *** when $p < 0.001$.

TEER values, which were generally lower than those in non-treated models and systemic application models (Table 2). TEER values after application with solvents and test chemicals were similar at each time point, indicating that the test chemicals *per se* were not causing any effect on this parameter. Although the application of chemicals to the surface of the EpiDerm™ was done carefully, it is likely that there was some mechanical disruption from the pipette and possibly also from the solvent (DMSO for permethrin and ethanol for hyperforin). This was more evident when test chemicals were repeatedly topically applied, in which the TEER values were lower after repeated than after single application.

3.2.2. *In-line measurements in the Chip2: LDH, glucose, lactate, albumin*

For all Chip2 experiments, the viability of the EpiDerm™ models and liver spheroids was measured by analyzing the medium for LDH, glucose, lactate and albumin content. Fig. 4 shows these measurements from repeated systemic and topical application of solvents (ethanol or DMSO) in both laboratories. There was a very good intra- and inter-laboratory reproducibility of all measurements after single and repeated systemic and topical application of solvents. The reproducibility was also observed for permethrin and hyperforin applications (Supplementary Fig. 1 and 2).

The percentage of total LDH released into the Chip2 circuit at each time point was very low (<4 % of the total amount in one circuit containing one EpiDerm™ model and 20 liver spheroids) in all systemically and topically treated and non-treated circuits in both laboratories (Fig. 4A). The total cumulative amount of LDH (in mU) released into the medium over 5 days was always less than 9 % of the total amount in the organoids. The release of LDH into the medium was unaffected by either test chemical (Supplementary Fig. 1 and 2).

The concentration of glucose in experiments performed in both laboratories was consistent over time and indicated that ~50 % of the concentration added was consumed by the organoids (Fig. 4B). In line with the consumption of glucose, the production of lactate was also generally consistent over time (Fig. 4C). The concentration of glucose and lactate in the medium was unaffected by either test chemical (Supplementary Fig. 1 and 2).

The values of human serum albumin in the medium were generally higher and more variable in measurements in Lab 1 than in Lab 2 (Fig. 4D); however, this was not due to the different kits used to measure albumin, since comparable values of the same test medium samples were measured using both kits (this was also true for glucose and lactate values, data not shown). The differences in the kits used was not considered to impact the results since both laboratories normalized the values to solvent control values; moreover, both measurements detected the decrease in albumin production caused by hyperforin (Supplementary Fig. 1). Importantly, the rate of albumin production in control circuits was maintained or increased over time in experiments from both laboratories (Fig. 4B). The production of albumin was unaffected by topical application of either test chemical (Supplementary Figs. 1 and 2) or by systemic and topical application of permethrin (Supplementary Fig. 2). A single application of hyperforin was considered non-toxic since initial albumin production values in these circuits were also lower (9.9 ± 1.8 mg/ml) than that measured in solvent control medium (11.5 ± 1.2 mg/ml) before its application.

In Lab 1, the systemic application of hyperforin resulted in a decrease in the % control albumin production after repeated systemic doses only (Supplementary Fig. 1A). In Lab 2, both single and repeated doses of hyperforin caused a decrease in % control albumin production (Supplementary Fig. 1A). After single application the production of albumin was maintained over 5 days (~2.5 μg/ml) and the % decrease was mainly due to control values increasing (from 2.3 ± 0.8 μg/ml on Day 1 to 4.9 ± 0.3 μg/ml on Day 5). By contrast, values in albumin production after repeated systemic application decreased over time, from 2.7 ± 0.7 μg/ml on Day 1 to 1.0 ± 0.3 μg/ml on Day 5. This effect was considered to reflect only minor toxicity since none of the other viability parameters (glucose consumption, lactate formation and LDH release) were affected by any treatment scenario of hyperforin (Supplementary Fig. 1).

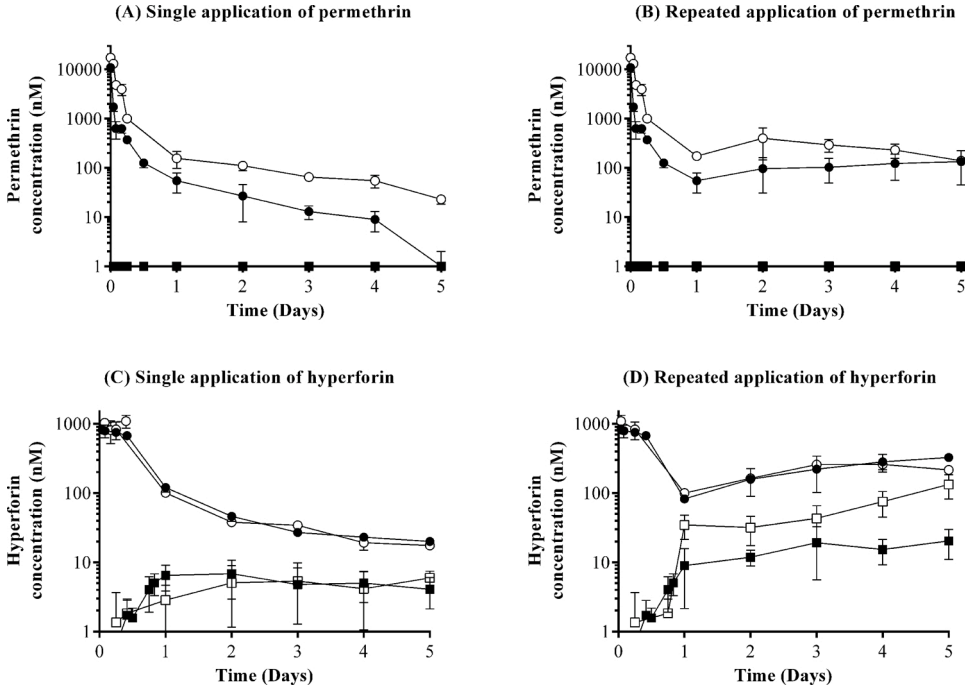

Fig. 5. Effect of application route and frequency: concentrations of permethrin (A and B) and hyperforin (C and D) in the Chip2 medium after a single (A and C) or repeated (B and D) systemic and topical application. Mean ± SD from 3 (Lab 2) and 5 (Lab 1) circuits are shown. Systemically (circles) and topically (squares) applied chemicals from Lab 1 (closed symbols) and Lab 2 (open symbols).

3.3. Chip2 experiments – test chemicals

3.3.1. Metabolism of parent chemicals

In the Chip2 experiments, the concentrations of the initial dosing solutions were measured to monitor the actual doses applied (unlike the pre-tests, which tested concentrations at the end of the incubations). While the same topical dose of permethrin was applied in both laboratories (~16 µM), the systemic dose was marginally different: 11 and 18 µM in Lab 1 and Lab 2, respectively. Notably, none of these actually reached the nominal target dose of 25 µM, which was likely to be due to the low solubility of this chemical and the difficulties in achieving complete dissolution of the solid.

The kinetics of the parent chemical, permethrin, after single and repeated systemic and topical application in both laboratories are shown in Fig. 5A and B. After systemic application, the concentration of permethrin rapidly decreased to 55 nM (Lab 1) and 175 nM (Lab 2) over the first 24 h (Fig. 5A). This was likely due to both non-specific binding and rapid metabolism, based on the pre-test incubations with empty

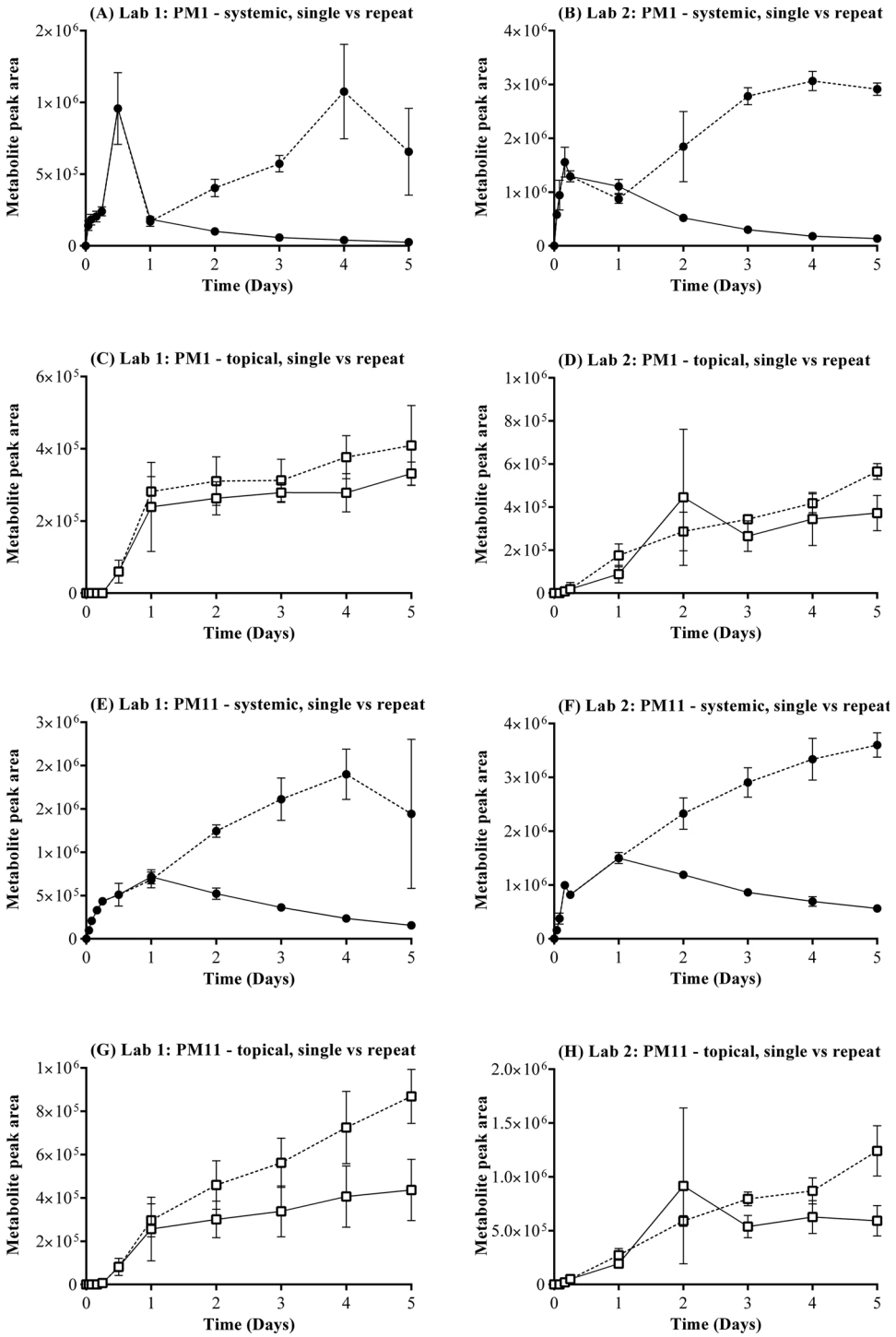

Fig. 6. Effect of application frequency: initial (PM1) and latent (PM11) permethrin metabolites present in the Chip2 after single (continuous line) and repeated (dotted line) systemic application in two laboratories. Solid lines depict single application and dotted lines depict repeated application of permethrin. Mean ± SD from 3 (Lab 2) and 5 (Lab 1) circuits are shown.

chips, as well as the production of metabolites during this time. The concentration of permethrin continued to decrease to 0 nM (Lab 1) and 23 nM (Lab 2) by Day 5 due to metabolism and its removal from the circuit due to the medium change (removing half the volume). Repeated application of permethrin resulted in higher concentrations in the medium over time, such that levels were 134 nM (Lab 1) and 140 nM (Lab 2) by Day 5 (Fig. 5B).

In contrast to the systemic route of application, permethrin was not detectable in the medium after topical application, as observed in both laboratories (Fig. 5A and B). This was in accordance with the pre-test, showing very little penetration of the parent compound through EpiDerm™ models into the medium. There was still no parent chemical present in the medium even after repeated application of permethrin (Fig. 5B).

After systemic application of hyperforin, >75 % of the applied dose remained in the medium 6–10 h later (Fig. 5C), in accordance with the relatively slow metabolism of this chemical observed in static incubations. The concentration continued to decrease over time from 100–120 nM on Day 1 to 17–20 nM on Day 5. As with permethrin, repeated application resulted in higher sustained concentrations of the parent chemical (325 nM compared to 20 nM in Lab 1 and 215 nM compared to 17 nM in Lab 2 after repeated and single systemic application, respectively) (Fig. 5D).

Unlike permethrin, a single topical application of hyperforin resulted

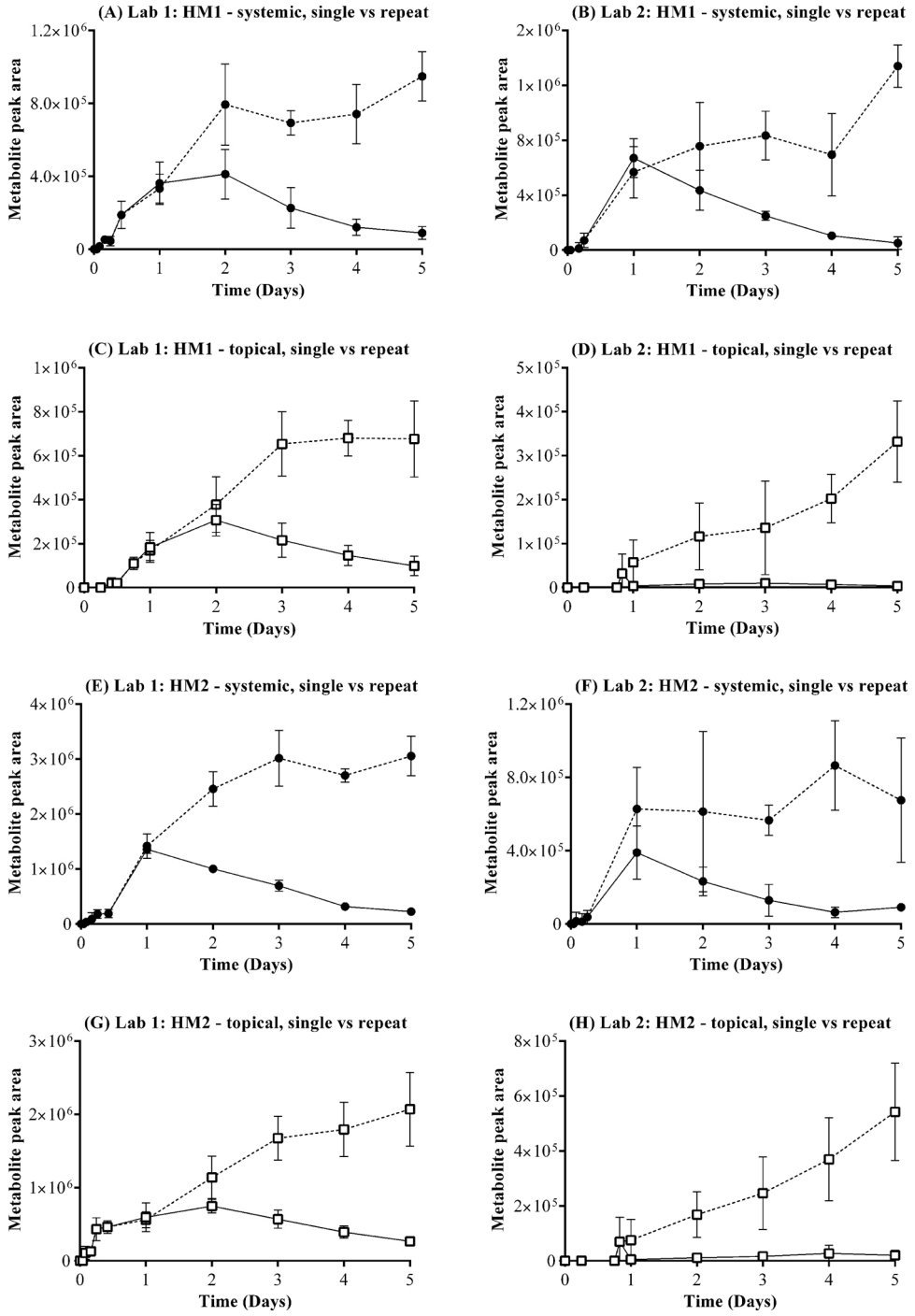

Fig. 7. Effect of application route and frequency: hyperforin single oxidized metabolites (HM1 and HM2). Values are peak areas. Mean ± SD from 3 (Lab 2) and 5 (Lab 1) circuits are shown. Solid lines depict single application and dotted lines depict repeated application of hyperforin.

in measurable levels in the systemic compartment, peaking on Day 1 (3−6 nM). The concentrations were much lower than the applied dose and the concentrations after systemic application (Fig. 5C). These findings were in accordance with the low but readily measurable penetration of hyperforin through EpiDerm™ models under static conditions, although the relative amount of hyperforin in the systemic circulation of the Chip2 after 24 h (0.5 % of the applied dose) was marginally lower than that in the static models (2 % of the applied dose (1 μM)). After repeated topical application, the amount of hyperforin gradually increased over time to levels close to those after systemic application on Day 5 in experiments in Lab 2 (133 nM and 215 nM after topic and systemic application, respectively) (Fig. 5D). The increase in hyperforin was also evident in experiments in Lab 1; however, concentrations after topical application only reached 20 nM on Day 5 (compared with 325 nM after systemic application).

3.3.2. *Metabolite formation*

The 12 metabolites of permethrin formed in static incubations with liver spheroids were also detected in the Chip2. To demonstrate the effect of route and dosing frequency, the production of only two permethrin metabolites detected in the medium after single and repeated systemic and topical application of permethrin in experiments from both laboratories are presented (Fig. 6). These metabolites represent a direct cleavage metabolite (PM1) and a conjugated metabolite formed after several transformations (PM11, the glucuronide of phenoxybenzoic acid). The profiles of these metabolites are typical for most of the metabolites detected and were comparable between the two laboratories (data not shown).

After single systemic application, PM1 was quickly formed, with a peak observed between 4 and 12 h, which subsequently decreased over the remaining 4 days (Fig. 6A and B). The level of PM1 in experiments from both Lab 1 and 2 increased between 1 and 4 h (both levels at 4 h were similar to that measured on Day 1); however, the marked high level of PM1 at 12 h observed in Lab 1 was not observed in Lab 2 most likely because no sample was taken at this time point in Lab 2. PM11 was more slowly formed than PM1, with a peak amount observed slightly later, at 24 h, possibly reflecting the sequential metabolism involved in its formation (Fig. 6E and F). Repeated systemic application of permethrin resulted in markedly increased levels of both metabolites than those observed after single application. The levels of PM1 and PM11 started to plateau by Day 4 after repeated application, suggesting a steady state concentration had been reached.

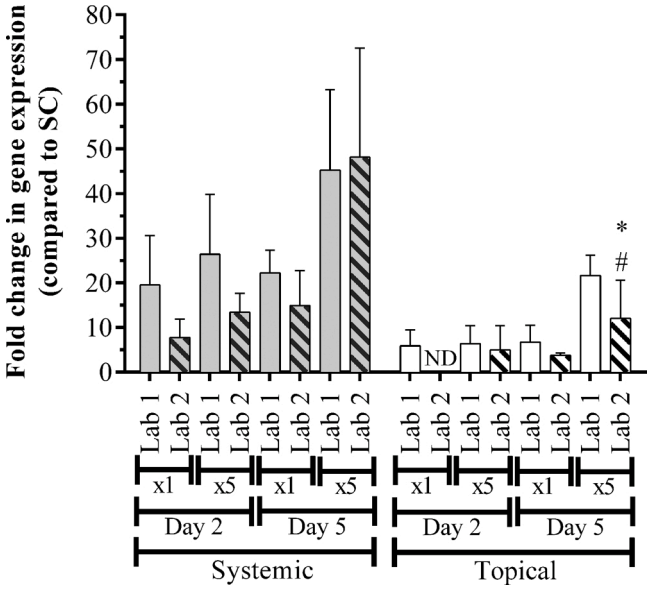

Fig. 8. CYP3A4 gene expression levels in liver spheroids after systemic and topical application of hyperforin in Chip2 experiments in Lab 1 and Lab 2. Mean ± SD from 3 (Lab 2) and 5 (Lab 1) circuits are shown. A statistical difference ($P < 0.05$) from the concurrent solvent control-treated liver spheroids is denoted by an asterisk and a statistical difference ($P < 0.05$) from the single application treated liver spheroids at the same time point is denoted by a hashtag.

Unlike the static EpiDerm™ penetration experiments in which no metabolites were formed, topical application in the Chip2 resulted in six permethrin metabolites detected in the medium from experiments from both laboratories. These included all the known *in vivo* metabolites shown in Fig. 1. Although the amounts of metabolites in the medium were not quantified, the peak areas of some the metabolites detected in the medium after topical application were on the same order of magnitude as those detected after systemic exposure. For example, after a single topical application of permethrin, the maximum peak areas of PM1, PM2, PM4, PM5, PM9 and PM11 were 107 %, 54 %, 79 %, 153 %, 40 % and 50 % of the maximum peak areas detected after systemic application. By contrast, other metabolites that were present in low amounts (according to the peak areas) after systemic application were not detected (or only in trace amounts) in the medium after topical application (PM3, PM6, PM7, PM8 and PM10).

Comparative analyses of single systemic and single topical permethrin exposure showed a clear difference in the kinetics of the main permethrin metabolites. While the concentrations of most metabolites peaked on Day 1 after systemic application, they gradually increased over 5 days after topical application. Repeated topical application did not increase the formation of PM1 and only marginally increased the formation of PM11. Interestingly, and in contrast to the systemic exposure route, levels of permethrin metabolites did not reach a plateau in the repeated topical application scenario.

Five metabolite peaks were detected after systemic and topical application of hyperforin and a sixth (HM4) was only detected after systemic application. Fig. 7 shows the production of two single oxidation metabolites of hyperforin detected in the medium after single and repeated systemic and topical application of permethrin. The kinetic profiles of these metabolites after systemic application were comparable in both laboratories. Concomitant with the slower depletion of parent chemical, there was a slow formation of hyperforin metabolites; whereby peak metabolite levels were observed between Days 1 and 2 after a single systemic application (Fig. 7A, B, E and F). Repeated systemic application of hyperforin caused the levels of both metabolites to continue to increase, reaching a maximum level on Day 2, which was sustained until Day 5.

Repeated topical application of hyperforin resulted in higher increasing levels of HM1 and HM2 over 5 days, evident in both laboratories. This reflected the increased amount of parent chemical also detected in the medium (Fig. 5C and D).

3.3.3. *Effect of test chemicals on XME expression – effect of application scenario*

Permethrin did not significantly alter (by more than 2-fold) any of the genes analyzed in liver spheroids at any of the time points measured (Day, 1, 2 and 5) under any dosing scenario (data not shown). By contrast, hyperforin induced a number of genes by more than 2-fold at one or more time points after systemic application. These included CYP3A4, ABCB1, UGT1A1 and PTGS2. The highest fold induction by hyperforin was observed with CYP3A4 (up to ~45-fold (Fig. 8), compared to 2- to 3-fold for other genes). Clear differences in the transcriptional response to hyperforin were observed in both laboratories for topical *versus* systemic application, whereby the CYP3A4 induction response was higher after systemic than after topical application (Fig. 8). This was also true for MDR1 (ABCB1) and UGT1A1, which were induced by ~2-fold on Day 2 after systemic application but was not induced after topical application (data not shown). The frequency of application also affected the CYP3A4 induction response; whereby the fold-induction on Day 5 was increased as a result of repeated application *via* both application routes.

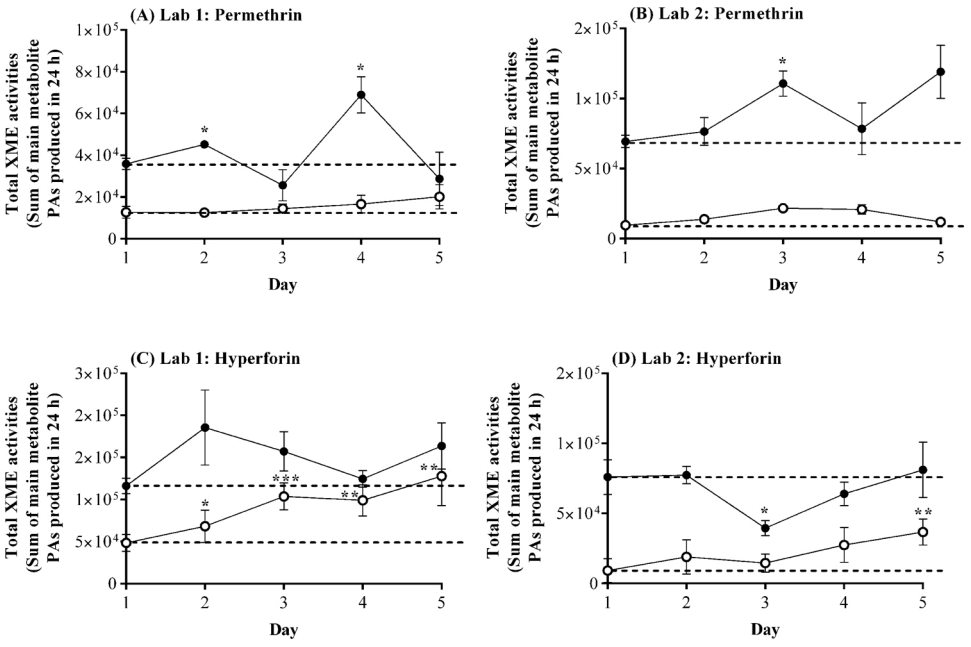

Fig. 9. XME activities of organoids in experiments measuring systemic (closed circles) and topical (open circles) application of permethrin and hyperforin in both laboratories. Open circles depict topical application and closed circles depict systemic application. The dotted lines denote the initial activities for each application scenario. Values on the y-axis are the mean ± SD of the sum of the increase in peak areas (PA) of all metabolites between the medium change and the following sample collection. A statistical difference from the Day 0 medium measurement is denoted with * when $p < 0.05$, with ** when $p < 0.01$ and *** when $p < 0.001$.

There were some genes that were decreased by more than 2-fold at one or more time points, which included albumin, CYP2A6 and CYP2E1. Albumin was selected as a marker for liver spheroid functionality. In the static incubations with liver spheroids, hyperforin was shown to decrease albumin secretion into the medium at higher concentrations, indicating that this chemical caused some toxicity or at least a slight decrease in hepatocyte functionality. Transcriptional analysis of the Chip2 experiments conducted in both laboratories indicated a decrease in albumin expression under conditions in which hyperforin may have accumulated in the systemic compartment *i.e.* repeated application over longer times, albeit to a small extent (ratios to solvent control of 0.70- and 0.67-fold in Lab 1 and 0.81 and 0.62-fold in Lab 2). This was reflected in the medium analysis of albumin in Chip2 experiments, which showed a decrease in albumin secretion on Day 2–5 after repeated systemic application of hyperforin (see Section 3.2.2 and Supplementary Fig. 2).

3.3.4. XME activities over time

Fig. 9 shows the calculated XME activities of organoids in experiments measuring systemic and topical application of permethrin and hyperforin in both laboratories. Total activities measured using permethrin reflect both Phase 1 and 2 XMEs; whereas, activities from hyperforin incubations reflect Phase 1 XMEs only (it was not metabolized to any phase 2 metabolites). With the exception of a single time point (Lab 2, hyperforin, Day 3, Fig. 9D), XME activities were not markedly lower than initial activities. Moreover, activities tended to be higher than initial values over time, notably when hyperforin was applied topically (demonstrated in both laboratories but statistically significant in Lab 1).

4. Discussion

In these preliminary proof-of concept studies evaluating the Chip2 for topically applied cosmetics ingredients, we have used the HUMIMIC Chip2, a multi-organ chip connecting EpiDerm™ models and liver spheroids to explore its applicability to provide information about the influence of application scenarios on the bioavailability and metabolic fate of two chemicals. Furthermore, proof of concept experiments were designed to evaluate other fundamental aspects of the use of MPS for risk assessment. These include transferability to other laboratories, intra-and inter-laboratory reproducibility, maintenance of the viability of the EpiDerm™ models and liver spheroids, and, in the case of the current studies, maintenance of XME activities. All these aspects were demonstrated in this study, from detection of medium viability markers to gene expression and parent/metabolite profiles.

Based on our results with permethrin and hyperforin, the Chip2 is suitable for testing compounds with a low solubility and high logP (~6). Artificial binding of chemicals to plastic materials and PDMS affects the free concentration of a chemical and consequently needs to be considered for dose finding, data interpretation and *in vitro in vivo* extrapolation, particularly for chemicals with a high logP such as permethrin and hyperforin (Groothuis et al., 2015; Wang et al., 2012). However, in the case of permethrin, metabolic stability tests indicated a rapid decline in cell-free incubations, whereas it was stable over 3 h when incubated with heat-inactivated cells. This indicates that the presence of protein in the incubation decreases non-specific binding to the PDMS. Protein was present in the Chip2 in the form of EpiDerm™ models and liver spheroids, thus allowing it to be available for metabolism. In addition, the binding to PDMS was also reversible, thus allowing it to be metabolized even if non-specific binding did occur. Therefore, matrix binding effects should be carefully evaluated in experiment-related context. Although hydrophobic molecules (logP >2.62) were reported to exhibit extensive adsorption to PDMS (Wang et al., 2012), other hydrophobic chemicals with LogP > 2.5, such as diethylstilbestrol, genistein and rhodamine 6 G were reported to show no binding to PDMS (Auner et al., 2019). Of note, the potential to enable topical application onto skin models may turn out as a major benefit of the MPS system to test insoluble compounds that pose major problems in standard 2D assays.

Skin models (native or reconstructed human epidermal) have been reported to be viable only for short durations *e.g.*, 2–3 days (Frasch and Barbero, 2018; Jacques et al., 2014); however, when native human skin or reconstructed human epidermal models were placed in trans-wells and cultured in the Chip2, they maintained a good structural architecture for 28 days (Wagner et al., 2013). We also demonstrated a good maintenance of EpiDerm™ models and liver spheroid functions over the entire incubation period. The EpiDerm™ model barrier function remained intact, according to histology, TEER measurements, media analyses, and the detection of proliferating cells in the basal layer even on Day 5 (according to Ki67 staining (Petrovic et al., 2018), data not shown). Daily applications of test chemicals to the EpiDerm™ surface

over 5 days were possible with no disruption of the barrier function and a minimal degree of disruption of the stratum. The liver spheroids were also well-maintained in the Chip2, as indicated by a low leakage of LDH, sustained glucose consumption and stable albumin production. We noted that albumin production, as a marker for primary hepatocyte functionality (Buyl et al., 2015), was the most sensitive marker for liver spheroid cytotoxicity, since other measurement, such as ATP decrease and LDH release, were only slightly altered at higher concentrations. Since the focus of these studies was on the metabolism of the two test chemicals, it was essential to demonstrate the maintenance of the metabolic competence of the organoids over time. This was assessed according to the production of permethrin and hyperforin metabolites between medium changes. The metabolic capacity of the liver spheroids was retained throughout the incubation, moreover, activities tended to increase over time. This increase was most notable when hyperforin was applied topically (a 2.6- and 4-fold increase in XME activities was demonstrated in Lab 1 and Lab 2, respectively), which are possibly due to CYP induction. Induction of functional XMEs (despite mRNA induction) may not be seen after repeated systemic application of hyperforin due to the minimal toxicity observed after Days 4 and 5. Increases in permethrin XME activities were not expected due to the lack of XME gene induction by this chemical.

Typically, *in vitro* screening assays for hepatic or skin metabolism are carried out using static incubations (Di et al., 2012; Eilstein et al., 2020; Genies et al., 2019). Ideally, MPS models should be able to demonstrate *in vivo* observations that static *in vitro* assays fail to reveal. This was the case for permethrin. After topical application to EpiDerm™ models in static culture, only trace amounts of parent chemical and no metabolites were detected in the medium after 48 h of incubation (0.06 % of the applied dose). By contrast, topical application in the Chip2 resulted in measurable levels of metabolites in the medium. Therefore, permethrin had clearly penetrated the EpiDerm™ models, although the parent chemical was not detected, presumably due to its extensive metabolism by the liver spheroids. Moreover, although the amounts of metabolites are only semi-quantitative, the peak areas of metabolites were not dissimilar to those after systemic exposure, suggesting considerably more than 0.06 % of the applied dose had penetrated. This was in accordance with predicted or measured *in vivo* human dermal absorption values for permethrin, which ranged from 0.5 % to 3.3 % of the applied dose (Ross et al., 2011; van der Rhee et al., 1989). Table 3 compares the conditions used in our experiments of static and dynamic incubations. These alone do not explain why there was such a difference between the results from static and dynamic incubations: (1) the medium was the same; therefore, there were no differences in sink conditions due to the presence of albumin in the medium; (2) the size (96-well) and batch of EpiDerm™ was the same; (3) the volume was 2-fold higher in dynamic incubations, which would decrease the sensitivity to detect metabolites in this model compared to static incubations; (4) the non-specific binding of permethrin in medium-only Chip2 circuits (to PDMS) was much higher than in polycarbonate culture plates used in the static experiments. While this may be expected to reduce the free fraction of permethrin and its metabolites (and the ability to detect them), the presence of the EpiDerm™ and the liver spheroids is likely to reduce non-specific binding, making it only a minor influencing factor (as was seen for the static incubation with heat-inactivated liver spheroids). Apart from the influence of the dynamic flow used in the Chip2, another factor that could have altered the penetration of permethrin was the level of occlusion. In static incubations the EpiDerm™ were semi-occluded with the plate lid and in the dynamic incubations, occlusion was complete (the compartment was closed using a screw lid). Occlusion could have increased the penetration of lipophilic permethrin (Hafeez and Maibach, 2013b); however, the logP is not predictive of whether a lipophilic chemical's penetration is enhanced by occlusion (Hafeez and Maibach, 2013a). Therefore, unless the effect of occlusion is specifically measured for permethrin, it is not possible to confirm this effect.

A higher extent of skin penetration of permethrin observed in the Chip2 experiments is consistent with human absorption studies, which estimate 2 % of the applied dose is excreted in the urine within 48 h of topical application, which is likely to be higher with ethanolic solvents (Committee on Toxicology, 1994). The accurate estimation of skin penetration is important in a safety assessment scenario. If static skin absorption studies had been used to estimate the systemic exposure of permethrin and its metabolites, they would have indicated little or no exposure, thus under-predicting the potential for systemic effects. This finding is especially important for permethrin since the parent chemical is neurotoxic and carcinogenic in laboratory animals at high doses (Committee on Toxicology, 1994) and one of its metabolites is an endocrine disruptor (Tyler et al., 2000). The rate of metabolism of pyrethroids are linked to their acute toxicity, such that rapidly hydrolyzed *trans* isomers are much less toxic than their *cis* analogues *i.e.* the parent chemical is responsible for neurotoxicity (Kaneko, 2011). Thus, an understanding of the metabolic fate of permethrin after absorption, regardless of the route, is useful. To investigate this further, we compared our findings with those of an *in vivo* human study in which permethrin was topically applied to the heads of healthy volunteers, followed by a 45 min wash (Tomalik-Scharte et al., 2005). This study confirmed that topically applied permethrin does enter the systemic circulation, based on the detection of its main metabolite, CVA (PM1 in our analyses), and its conjugates in the urine. While the Chip2 used in this study does not incorporate a renal compartment, the excretion could be considered to be in the form of the medium change carried out on a daily basis. Despite this caveat, the profile of CVA/PM1 "excreted" in the Chip2 circuit was remarkably similar to the urinary excreted amount, resembling a peak excretion at 24 h that slowly declined over the remaining 4 days. This supports the added value of Chip2 experiments to safety assessment by providing *in vivo*-relevant estimates for the rate of metabolite formation and clearance over time.

An advantage of the Chip2 is its potential to determine the effect of repeated application of chemicals over prolonged periods. We observed clear differences in the kinetics of the main permethrin and hyperforin metabolites after single and repeated systemic exposure. After a single application, the concentrations of metabolites peaked on Day 1 (permethrin) or 2 (hyperforin) and then decreased over the following days. By contrast, after repeated systemic application, the levels of metabolites increased gradually over time, reaching near maximal levels by Day 5. Interestingly, while repeated topical application of hyperforin resulted in higher levels of its metabolites over time compared to a single dose, this was not the case for permethrin. This could be related to the relative amount of parent chemical entering the circuit, which were measurable and increased (from ~6 nM to 35−133 nM) after repeated application of hyperforin; whereas, parent permethrin was not detected in the medium after single or repeated topical application. Importantly, the latter observation suggests that despite repeated application, metabolic pathways in the liver would not be saturated under this dosing scenario; therefore, the fast detoxification by the liver limits the exposure of the systemic circulation to permethrin parent chemical. This is important for risk assessments because parent permethrin is neurotoxic (Committee on Toxicology, 1994).

In addition to evaluating the effect of the dosing scenario on the metabolic fate of chemicals, the effect of the test chemicals on the organoids can be evaluated in the same experiment. Here, we concentrated on analyzing the effect on XMEs in liver spheroids, since permethrin and hyperforin are both known to activate PXR (Lemaire et al., 2006; Moore et al., 2000) and induce CYPs in 2D *in vitro* hepatic models (Das et al., 2008; Jackson et al., 2014; Komoroski et al., 2004). Das et al. (2008) showed that 100 μM permethrin induced CYP1A1, CYP3A4, CYP3A5, CYP2B6 and CYP2A6 mRNA in human hepatocytes; however, the extent of induction was low and variable. We showed that a lower dose of 25 μM permethrin did not induce the expression of these CYPs in static culture or Chip2 incubations. This suggests that this pesticide at this concentration would not pose a risk of altering the metabolism of other co-exposed chemicals, especially not *via* the topical

route, since our results imply negligible plasma concentrations of permethrin due to the impact of skin barrier function and fast liver clearance.

Hyperforin is a known inducer of CYP3A4 in human hepatocytes *in vitro* [49] and in humans (Linde et al., 1996; Wheatley, 1997). In addition to being used for oral treatment of depression, hyperforin (in St John's Wort extracts) is used topically due to its beneficial antioxidant, anti-inflammatory, anticancer, and antimicrobial activities (Wolfle et al., 2014). While primary human hepatocyte-based induction studies may facilitate the detection of CYP3A4 induction, they do not evaluate exposure scenario-dependent differences in XME modulation. As indicated by the static incubations with EpiDerm™ models, there was some CYP-dependent first-pass metabolism of hyperforin in the skin, which along with the barrier function, likely affects its bioavailability and, thus, its systemic effects *i.e.* on the liver spheroids. In accordance with this hypothesis, our results indicated that the induction of CYP3A4 mRNA was lower at all time points after topical than systemic application of hyperforin. In addition, the fold induction of CYP3A4 was highest on Day 5 after repeated dose applications. These differences were likely to be due to the respective systemic concentrations of parent hyperforin *e.g.* on Day 1 after a single application, the concentration of hyperforin was 3−6 nM after topical application and 100−120 nM after systemic application; and on Day 5 after systemic application, the concentration of hyperforin was 18−20 nM after a single application and 214−325 nM after repeated application. Notably, the concentrations measured in the Chip2 were relevant to steady state *in vivo* human plasma concentrations causing CYP3A4 induction, which are reported to be ~180 nM after three daily oral doses of 300 mg hyperforin (Biber et al., 1998).

5. Conclusions

In conclusion, our results demonstrate the reproducibility, reliability, robustness, and relevance of the Chip2 using the example of investigating the effect of dosing scenarios on the metabolism of two test chemicals. The technology and expertise in handling the system were transferrable to a second laboratory and the results were reproducible within and across both laboratories. Importantly, the viability of EpiDerm™ models and liver spheroids and the XME capacity of the liver spheroids were shown to be maintained during the entire course of the 6-day experiment. We demonstrate this *in vitro* model is relevant and valuable to provide information on potential *in vivo* effects. While it is understood that this empirical model cannot mimic the complex *in vivo* human physiology, it can be used as a tool for safety assessment to provide information on the metabolic fate of a chemical after topical and systemic application.

Funding sources

This work was supported by Cosmetics Europe, Brussels, Belgium.

Declaration of Competing Interest

The authors report no declarations of interest.

Acknowledgement

This work was funded by Cosmetics Europe.

Appendix A. Supplementary data

Supplementary material related to this article can be found, in the online version, at doi:https://doi.org/10.1016/j.tox.2020.152637.

References

Ackermann, K., Borgia, S.L., Korting, H.C., Mewes, K.R., Schäfer-Korting, M., 2010. The Phenion full-thickness skin model for percutaneous absorption testing. Skin Pharmacol. Physiol. 23, 105–112.

Atac, B., Wagner, I., Horland, R., Lauster, R., Marx, U., Tonevitsky, A.G., Azar, R.P., Lindner, G., 2013. Skin and hair on-a-chip: in vitro skin models versus ex vivo tissue maintenance with dynamic perfusion. Lab Chip 13, 3555–3561.

Auner, A.W., Tasneem, K.M., Markov, D.A., McCawley, L.J., Hutson, M.S., 2019. Chemical-PDMS binding kinetics and implications for bioavailability in microfluidic devices. Lab Chip 19, 864–874.

Berggren, E., White, A., Ouedraogo, G., Paini, A., Richarz, A.N., Bois, F.Y., Exner, T., Leite, S., Grunsven, L.A.V., Worth, A., Mahony, C., 2017. Ab initio chemical safety assessment: a workflow based on exposure considerations and non-animal methods. Comput Toxicol 4, 31–44.

Biber, A., Fischer, H., Romer, A., Chatterjee, S.S., 1998. Oral bioavailability of hyperforin from hypericum extracts in rats and human volunteers. Pharmacopsychiatry 31 (Suppl 1), 36–43.

Buyl, K., De Kock, J., Bolleyn, J., Rogiers, V., Vanhaecke, T., 2015. Measurement of albumin secretion as functionality test in primary hepatocyte cultures. Methods Mol. Biol. 1250, 303–308.

Chapman, K.E., Thomas, A.D., Wills, J.W., Pfuhler, S., Doak, S.H., Jenkins, G.J., 2014. Automation and validation of micronucleus detection in the 3D EpiDerm human reconstructed skin assay and correlation with 2D dose responses. Mutagenesis 29, 165–175.

Choi, J., Rose, R.L., Hodgson, E., 2002. In vitro human metabolism of permethrin: the role of human alcohol and aldehyde dehydrogenases. Pestic. Biochem. Physiol. 74, 117–128.

Committee on Toxicology, 1994. Health Effects of Permethrin-Impregnated Army Battle-Dress Uniforms. The National Academies Press, Washington, DC.

Das, P.C., Streit, T.M., Cao, Y., Rose, R.L., Cherrington, N., Ross, M.K., Wallace, A.D., Hodgson, E., 2008. Pyrethroids: cytotoxicity and induction of CYP isoforms in human hepatocytes. Drug Metabol. Drug Interact. 23, 211–236.

Di, L., Keefer, C., Scott, D.O., Strelevitz, T.J., Chang, G., Bi, Y.A., Lai, Y., Duckworth, J., Fenner, K., Troutman, M.D., Obach, R.S., 2012. Mechanistic insights from comparing intrinsic clearance values between human liver microsomes and hepatocytes to guide drug design. Eur. J. Med. Chem. 57, 441–448.

Edington, C.D., Chen, W.L.K., Geishecker, E., Kassis, T., Soenksen, L.R., Bhushan, B.M., Freake, D., Kirschner, J., Maass, C., Tsamandouras, N., Valdez, J., Cook, C.D., Parent, T., Snyder, S., Yu, J., Suter, E., Shockley, M., Velazquez, J., Velazquez, J.J., Stockdale, L., Papps, J.P., Lee, I., Vann, N., Gamboa, M., LaBarge, M.E., Zhong, Z., Wang, X., Boyer, L.A., Lauffenburger, D.A., Carrier, R.L., Communal, C., Tannenbaum, S.R., Stokes, C.L., Hughes, D.J., Rohatgi, G., Trumper, D.L., Cirit, M., Griffith, L.G., 2018. Interconnected microphysiological systems for quantitative biology and pharmacology studies. Sci. Rep. 8, 4530.

Eilstein, J., Gregoire, S., Fabre, A., Arbey, E., Genies, C., Duplan, H., Rothe, H., Ellison, C., Cubberley, R., Schepky, A., Lange, D., Klaric, M., Hewitt, N.J., Jacques-Jamin, C., 2020. Use of human liver and EpiSkin S9 subcellular fractions as a screening assays to compare the in vitro hepatic and dermal metabolism of 47 cosmetics-relevant chemicals. J. Appl. Toxicol.

EU, 2009. Regulation (EC) No 1223/2009 of the European Parliament and of the Council of 30 November 2009 on Cosmetic Products. Retrieved from. http://data.europa.eu/eli/reg/2009/1223/oj.

Frasch, H.F., Barbero, A.M., 2018. In vitro human skin permeation of benzene in gasoline: effects of concentration, multiple dosing and skin preparation. J. Expo. Sci. Environ. Epidemiol. 28, 193–201.

Friedman, S.L., 2008. Hepatic stellate cells: protean, multifunctional, and enigmatic cells of the liver. Physiol. Rev. 88, 125–172.

Genies, C., Jamin, E.L., Debrauwer, L., Zalko, D., Person, E.N., Eilstein, J., Gregoire, S., Schepky, A., Lange, D., Ellison, C., Roe, A., Salhi, S., Cubberley, R., Hewitt, N.J., Rothe, H., Klaric, M., Duplan, H., Jacques-Jamin, C., 2019. Comparison of the metabolism of 10 chemicals in human and pig skin explants. J. Appl. Toxicol. 39, 385–397.

Gordon, S., Daneshian, M., Bouwstra, J., Caloni, F., Constant, S., Davies, D.E., Dandekar, G., Guzman, C.A., Fabian, E., Haltner, E., Hartung, T., Hasiwa, N., Hayden, P., Kandarova, H., Khare, S., Krug, H.F., Kneuer, C., Leist, M., Lian, G., Marx, U., Metzger, M., Ott, K., Prieto, P., Roberts, M.S., Roggen, E.L., Tralau, T., van den Braak, C., Walles, H., Lehr, C.M., 2015. Non-animal models of epithelial barriers (skin, intestine and lung) in research, industrial applications and regulatory toxicology. Altex 32, 327–378.

Gotz, C., Hewitt, N.J., Jermann, E., Tigges, J., Kohne, Z., Hubenthal, U., Krutmann, J., Merk, H.F., Fritsche, E., 2012. Effects of the genotoxic compounds, benzo[a]pyrene and cyclophosphamide on phase 1 and 2 activities in EpiDerm models. Xenobiotica 42, 526–537.

Groothuis, F.A., Heringa, M.B., Nicol, B., Hermens, J.L.M., Blaauboer, B.J., Kramer, N.I., 2015. Dose metric considerations in in vitro assays to improve quantitative in vitro-in vivo dose extrapolations. Toxicology 332, 30–40.

Hafeez, F., Maibach, H., 2013a. Do partition coefficients (liphophilicity/hydrophilicity) predict effects of occlusion on percutaneous penetration in vitro: a retrospective review. Cutan. Ocul. Toxicol. 32, 299–303.

Hafeez, F., Maibach, H., 2013b. Occlusion effect on in vivo percutaneous penetration of chemicals in man and monkey: partition coefficient effects. Skin Pharmacol. Physiol. 26, 85–91.

Hart, S.N., Li, Y., Nakamoto, K., Subileau, E.A., Steen, D., Zhong, X.B., 2010. A comparison of whole genome gene expression profiles of HepaRG cells and HepG2

cells to primary human hepatocytes and human liver tissues. Drug Metab. Dispos. 38, 988–994.
Hasenberg, T., Mühleder, S., Dotzler, A., Bauer, S., Labuda, K., Holnthoner, W., Redl, H., Lauster, R., Marx, U., 2015. Emulating human microcapillaries in a multi-organ-chip platform. J. Biotechnol. 216, 1–10.
Hedges, L., Brown, S., MacLeod, A.K., Vardy, A., Doyle, E., Song, G., Moreau, M., Yoon, M., Osimitz, T.G., Lake, B.G., 2019. Metabolism of deltamethrin and cis- and trans-permethrin by human expressed cytochrome P450 and carboxylesterase enzymes. Xenobiotica 49, 521–527.
Hewitt, N.J., Edwards, R.J., Fritsche, E., Goebel, C., Aeby, P., Scheel, J., Reisinger, K., Ouedraogo, G., Duche, D., Eilstein, J., Latil, A., Kenny, J., Moore, C., Kuehnl, J., Barroso, J., Fautz, R., Pfuhler, S., 2013. Use of human in vitro skin models for accurate and ethical risk assessment: metabolic considerations. Toxicol. Sci. 133, 209–217.
Higashi, T., Friedman, S.L., Hoshida, Y., 2017. Hepatic stellate cells as key target in liver fibrosis. Adv. Drug Deliv. Rev. 121, 27–42.
Hokkanen, J., Tolonen, A., Mattila, S., Turpeinen, M., 2011. Metabolism of hyperforin, the active constituent of St. John's wort, in human liver microsomes. Eur. J. Pharm. Sci. 42, 273–284.
Hübner, J., Raschke, M., Rutschle, I., Grassle, S., Hasenberg, T., Schirrmann, K., Lorenz, A., Schnurre, S., Lauster, R., Maschmeyer, I., Steger-Hartmann, T., Marx, U., 2018. Simultaneous evaluation of anti-EGFR-induced tumour and adverse skin effects in a microfluidic human 3D co-culture model. Sci. Rep. 8, 15010.
Jackson, J.P., Freeman, K., Hatfield, J., St. Claire, B., Hubert, C., Brouwer, K.R., 2014. Qualyst transporter solutions. In vitro strategy to quantify changes in hepatobiliary drug clearance by herbal extracts. ASP Meeting.
Jacques, C., Perdu, E., Jamin, E.L., Cravedi, J.P., Mavon, A., Duplan, H., Zalko, D., 2014. Effect of skin metabolism on dermal delivery of testosterone: qualitative assessment using a new short-term skin model. Skin Pharmacol. Physiol. 27, 188.
Jetten, M.J., Kleinjans, J.C., Claessen, S.M., Chesne, C., van Delft, J.H., 2013. Baseline and genotoxic compound induced gene expression profiles in HepG2 and HepaRG compared to primary human hepatocytes. Toxicol. In Vitro 27, 2031–2040.
Kaneko, H., 2011. Pyrethroids: mammalian metabolism and toxicity. J. Agric. Food Chem. 59, 2786–2791.
Komoroski, B.J., Zhang, S., Cai, H., Hutzler, J.M., Frye, R., Tracy, T.S., Strom, S.C., Lehmann, T., Ang, C.Y., Cui, Y.Y., Venkataramanan, R., 2004. Induction and inhibition of cytochromes P450 by the St. John's wort constituent hyperforin in human hepatocyte cultures. Drug Metab. Dispos. 32, 512–518.
Lavado, R., Li, J., Rimoldi, J.M., Schlenk, D., 2014. Evaluation of the stereoselective biotransformation of permethrin in human liver microsomes: contributions of cytochrome P450 monooxygenases to the formation of estrogenic metabolites. Toxicol. Lett. 226, 192–197.
Lee, J.-y., Duke, R.K., Tran, V.H., Hook, J.M., Duke, C.C., 2006. Hyperforin and its analogues inhibit CYP3A4 enzyme activity. Phytochemistry 67, 2550–2560.
Lemaire, G., Mnif, W., Pascussi, J.M., Pillon, A., Rabenoelina, F., Fenet, H., Gomez, E., Casellas, C., Nicolas, J.C., Cavailles, V., Duchesne, M.J., Balaguer, P., 2006. Identification of new human pregnane X receptor ligands among pesticides using a stable reporter cell system. Toxicol. Sci. 91, 501–509.
Liebsch, M., Barrabas, C., Traue, D., Spielmann, H., 1997. Development of a new in vitro test for dermal phototoxicity using a model of reconstituted human epidermis. Altex 14, 165–174.
Linde, K., Ramirez, G., Mulrow, C.D., Pauls, A., Weidenhammer, W., Melchart, D., 1996. St John's wort for depression–an overview and meta-analysis of randomised clinical trials. Bmj 313, 253–258.
Maass, C., Stokes, C.L., Griffith, L.G., Cirit, M., 2017. Multi-functional scaling methodology for translational pharmacokinetic and pharmacodynamic applications using integrated microphysiological systems (MPS). Integr. Biol. (Camb) 9, 290–302.
Marx, U., Andersson, T.B., Bahinski, A., Beilmann, M., Beken, S., Cassee, F.R., Cirit, M., Daneshian, M., Fitzpatrick, S., Frey, O., Gaertner, C., Giese, C., Griffith, L., Hartung, T., Heringa, M.B., Hoeng, J., de Jong, W.H., Kojima, H., Kuehnl, J., Leist, M., Luch, A., Maschmeyer, I., Sakharov, D., Sips, A.J., Steger-Hartmann, T., Tagle, D.A., Tonevitsky, A., Tralau, T., Tsyb, S., van de Stolpe, A., Vandebriel, R., Vulto, P., Wang, J., Wiest, J., Rodenburg, M., Roth, A., 2016. Biology-inspired microphysiological system approaches to solve the prediction dilemma of substance testing. Altex 33, 272–321.
Maschmeyer, I., Hasenberg, T., Jaenicke, A., Lindner, M., Lorenz, A.K., Zech, J., Garbe, L. A., Sonntag, F., Hayden, P., Ayehunie, S., Lauster, R., Marx, U., Materne, E.M., 2015a. Chip-based human liver-intestine and liver-skin co-cultures–A first step toward systemic repeated dose substance testing in vitro. Eur. J. Pharm. Biopharm. 95, 77–87.
Maschmeyer, I., Lorenz, A.K., Schimek, K., Hasenberg, T., Ramme, A.P., Hubner, J., Lindner, M., Drewell, C., Bauer, S., Thomas, A., Sambo, N.S., Sonntag, F., Lauster, R., Marx, U., 2015b. A four-organ-chip for interconnected long-term co-culture of human intestine, liver, skin and kidney equivalents. Lab Chip 15, 2688–2699.
Materne, E.M., Ramme, A.P., Terrasso, A.P., Serra, M., Alves, P.M., Brito, C., Sakharov, D.A., Tonevitsky, A.G., Lauster, R., Marx, U., 2015. A multi-organ chip co-culture of neurospheres and liver equivalents for long-term substance testing. J. Biotechnol. 205, 36–46.
Moore, L.B., Goodwin, B., Jones, S.A., Wisely, G.B., Serabjit-Singh, C.J., Willson, T.M., Collins, J.L., Kliewer, S.A., 2000. St. John's wort induces hepatic drug metabolism through activation of the pregnane X receptor. Proc Natl Acad Sci U S A 97, 7500–7502.
Mufti, N.A., Bleckwenn, N.A., Babish, J.G., Shuler, M.L., 1995. Possible involvement of the Ah receptor in the induction of cytochrome P-450IA1 under conditions of hydrodynamic shear in microcarrier-attached hepatoma cell lines. Biochem. Biophys. Res. Commun. 208, 144–152.
Obach, R.S., 2000. Inhibition of human cytochrome P450 enzymes by constituents of St. John's Wort, an herbal preparation used in the treatment of depression. J. Pharmacol. Exp. Ther. 294, 88–95.
OECD, 2017. Test No. 437: Bovine Corneal Opacity and Permeability Test Method for Identifying i) Chemicals Inducing Serious Eye Damage and ii) Chemicals Not Requiring Classification for Eye Irritation or Serious Eye Damage.
OECD, 2018. Test No. 491: Short Time Exposure In Vitro Test Method for Identifying i) Chemicals Inducing Serious Eye Damage and ii) Chemicals Not Requiring Classification for Eye Irritation or Serious Eye Damage.
OECD, 2019a. Test No. 431: in Vitro Skin Corrosion: Reconstructed Human Epidermis (RHE) Test Method.
OECD, 2019b. Test No. 439: In Vitro Skin Irritation: Reconstructed Human Epidermis Test Method.
Pal, D., Mitra, A.K., 2006. MDR- and CYP3A4-mediated drug-herbal interactions. Life Sci. 78, 2131–2145.
Park, J., Li, Y., Berthiaume, F., Toner, M., Yarmush, M.L., Tilles, A.W., 2008. Radial flow hepatocyte bioreactor using stacked microfabricated grooved substrates. Biotechnol. Bioeng. 99, 455–467.
Petrovic, A., Petrovic, V., Milojkovic, B., Nikolic, I., Jovanovic, D., Antovic, A., Milic, M., 2018. Immunohistochemical distribution of Ki67 in epidermis of thick glabrous skin of human digits. Arch. Dermatol. Res. 310, 85–93.
Portes, P., Pygmalion, M.J., Popovic, E., Cottin, M., Mariani, M., 2002. Use of human reconstituted epidermis Episkin for assessment of weak phototoxic potential of chemical compounds. Photodermatol. Photoimmunol. Photomed. 18, 96–102.
Puche, J.E., Saiman, Y., Friedman, S.L., 2013. Hepatic stellate cells and liver fibrosis. Compr. Physiol. 3, 1473–1492.
Ramaiahgari, S.C., Ferguson, S.S., 2019. Organotypic 3D HepaRG liver model for assessment of drug-induced cholestasis. Methods Mol. Biol. 1981, 313–323.
Ramaiahgari, S.C., Waidyanatha, S., Dixon, D., DeVito, M.J., Paules, R.S., Ferguson, S.S., 2017. From the cover: three-dimensional (3D) HepaRG spheroid model with physiologically relevant xenobiotic metabolism competence and hepatocyte functionality for liver toxicity screening. Toxicol. Sci. 159, 124–136.
Reisinger, K., Blatz, V., Brinkmann, J., Downs, T.R., Fischer, A., Henkler, F., Hoffmann, S., Krul, C., Liebsch, M., Luch, A., Pirow, R., Reus, A.A., Schulz, M., Pfuhler, S., 2018. Validation of the 3D Skin Comet assay using full thickness skin models: Transferability and reproducibility. Mutat. Res. Genet. Toxicol. Environ. Mutagen. 827, 27–41.
Reisinger, K., Dony, E., Wolf, T., Maul, K., 2019. Hen's egg test for micronucleus induction (HET-MN). Methods Mol. Biol. 2031, 195–208.
Ross, J.H., Reifenrath, W.G., Driver, J.H., 2011. Estimation of the percutaneous absorption of permethrin in humans using the parallelogram method. J. Toxicol. Environ. Health Part A 74, 351–363.
Saxena, A., Tripathi, K.P., Roy, S., Khan, F., Sharma, A., 2008. Pharmacovigilance: effects of herbal components on human drugs interactions involving cytochrome P450. Bioinformation 3, 198–204.
Schimek, K., Busek, M., Brincker, S., Groth, B., Hoffmann, S., Lauster, R., Lindner, G., Lorenz, A., Menzel, U., Sonntag, F., Walles, H., Marx, U., Horland, R., 2013. Integrating biological vasculature into a multi-organ-chip microsystem. Lab Chip 13, 3588–3598.
Sung, J.H., Shuler, M.L., 2009. A micro cell culture analog (microCCA) with 3-D hydrogel culture of multiple cell lines to assess metabolism-dependent cytotoxicity of anti-cancer drugs. Lab Chip 9, 1385–1394.
Tilles, A.W., Baskaran, H., Roy, P., Yarmush, M.L., Toner, M., 2001. Effects of oxygenation and flow on the viability and function of rat hepatocytes cocultured in a microchannel flat-plate bioreactor. Biotechnol. Bioeng. 73, 379–389.
Tomalik-Scharte, D., Lazar, A., Meins, J., Bastian, B., Ihrig, M., Wachall, B., Jetter, A., Tantcheva-Poor, I., Mahrle, G., Fuhr, U., 2005. Dermal absorption of permethrin following topical administration. Eur. J. Clin. Pharmacol. 61, 399–404.
Truskey, G.A., 2018. Human microphysiological systems and organoids as in vitro models for toxicological studies. Front. Public Health 6, 185.
Tyler, C.R., Beresford, N., Van der Woning, M., Sumpter, J.P., Thorpe, K., 2000. Metabolism and environmental degradation of pyrethroid insecticides produce compounds with endocrine activities. Environ. Toxicol. Chem. 19, 801.
van der Rhee, H.J., Farquhar, J.A., Vermeulen, N.P., 1989. Efficacy and transdermal absorption of permethrin in scabies patients. Acta Derm. Venereol. 69, 170–173.
Van Ness, K.P., Chang, S.Y., Weber, E.J., Zumpano, D., Eaton, D.L., Kelly, E.J., 2017. Microphysiological systems to assess nonclinical toxicity. Curr. Protoc. Toxicol. 73, 14.18.11-14.18.28.
Vinci, B., Duret, C., Klieber, S., Gerbal-Chaloin, S., Sa-Cunha, A., Laporte, S., Suc, B., Maurel, P., Ahluwalia, A., Daujat-Chavanieu, M., 2011. Modular bioreactor for primary human hepatocyte culture: medium flow stimulates expression and activity of detoxification genes. Biotechnol. J. 6, 554–564.
Wagner, I., Materne, E.M., Brincker, S., Sussbier, U., Fradrich, C., Busek, M., Sonntag, F., Sakharov, D.A., Trushkin, E.V., Tonevitsky, A.G., Lauster, R., Marx, U., 2013.

A dynamic multi-organ-chip for long-term cultivation and substance testing proven by 3D human liver and skin tissue co-culture. Lab Chip 13, 3538–3547.
Wang, J.D., Douville, N.J., Takayama, S., ElSayed, M., 2012. Quantitative analysis of molecular absorption into PDMS microfluidic channels. Ann. Biomed. Eng. 40, 1862–1873 [PubMed: 22484830].
Wang, Z., Luo, X., Anene-Nzelu, C., Yu, Y., Hong, X., Singh, N.H., Xia, L., Liu, S., Yu, H., 2015. HepaRG culture in tethered spheroids as an in vitro three-dimensional model for drug safety screening. J. Appl. Toxicol. 35, 909–917.
Wheatley, D., 1997. LI 160, an extract of St. John's wort, versus amitriptyline in mildly to moderately depressed outpatients–a controlled 6-week clinical trial. Pharmacopsychiatry 30 (Suppl 2), 77–80.
Wolfle, U., Seelinger, G., Schempp, C.M., 2014. Topical application of st. John's wort (Hypericum perforatum). Planta Med 80, 109–120.